Bull. nat. Hist. Mus. Lond. (Geol.) **49**(2): 81–98 Issued 25 November 1993

Mobility and fixation of a variety of elements, in particular boron, during the metasomatic development of adinoles at Dinas Head, Cornwall

C.T. WILLIAMS, R.F. SYMES and V.K. DIN

Department of Mineralogy, The Natural History Museum, Cromwell Road, London SW7 5BD, U.K.

Synopsis. A geochemical investigation of adinoles and related spilositic rocks from Dinas Head, Cornwall, has been undertaken in an attempt to clarify the relationship between these altered sediments and associated doleritic intrusions. Comparisons are made with other similar dolerite/sediment associations from northern Cornwall. Data for a wide range of major, minor and trace elements are presented for the various rock types observed, and the mobility, fixation and correlations for several elements during the adinolisation process discussed. Boron distribution maps, obtained by particle track analysis, and boron isotope ratios were used in an attempt to identify the potential source of the boron for the tourmalinisation of one suite of rocks in the area.

INTRODUCTION

As part of a programme to study mobility and fixation of trace elements during metasomatic (fluid) movement between igneous and associated sedimentary rocks, a geochemical study of the adinoles of the Dinas Head area, N. Cornwall has been made. This paper reports the results of this study.

Dinas Head is a small headland (GR SW 848,762), part of the Trevose Head promontory which lies some five miles west of Padstow on the north coast of Cornwall (Fig. 1). The area of Trevose Head (Dinas Head) is formed from a thick sequence of Upper Devonian sediments, mostly shales (now slates) and thinner carbonate-rich horizons. These beds were substantially deformed by Variscan earth movements so that some areas are extensively folded and faulted. However, despite this deformation, excellent thick series of spilosites and adinoles are exposed in the relatively steep cliffs of the headland, although no one band (or bed) of sediment can be traced with certainty into its metasomatised equivalent. Exposure is poor on the grass covered plateau at the top of the headland.

This sequence has been extensively intruded by massive dolerite sills, which form large 'greenstone' units at the base of the cliffs with minor stringers intruding parts of the rest of the sequence. The intrusion of these dolerites has been suggested as the cause of formation of the spilosites and adinoles of this area. The area has recently been remapped by a combined BGS/Exeter University team and will be published as 1:50,000 Geological Survey Sheet 335/336 (Trevose Head and Camelford).

BACKGROUND

The term adinole was first defined for rocks from the Harz Mountains of Germany by Kayser (1870) and first used for British rocks by Teall (1888) for rocks from the Tremadoc area of Wales. Often a crude relationship can be described such that the sequence adinole-spilosite-desmosite-unaltered shale represents increasing distance from contact with a basic igneous intrusion.

In the literature adinoles are usually described as massive, compact, featureless, white-weathering rocks consisting of a fine-grained mosaic of albite and quartz (often with minor carbonate). Spilosites have a distinctive 'spotted' texture and a fine-grained sericitic matrix, with chlorite and quartz, while desmosites, although formed from the same minerals as spilosites, tend to be banded rather than spotted.

The albite-rich rocks developed between the dolerite (greenstone) and shales of Dinas Head were first recognised as possible adinoles by Fox (1895). He questioned whether the soda-feldspar rocks (as he described them) were meta-igneous, and not metasediments, being originally keratophyric lavas or tuffs. However, he described spherulitic structures seen in one outcrop as apparently of igneous origin but concluded that they were metasomatised sediments. McMahon and Hutchings (1895) believed the spherulitic structure developed in the adinoles at Dinas Head to be a product of contact metamorphism. Dewey (1915) considered that the composition of the slate into which the dolerites were intruded affects the products of such metamorphism/metasomatism. He suggested that the iron content (and thus colour) of the original shales determines whether they become adinoles or not — such that purple, red or green shales (slates) rich in iron tend to develop spots (spilosites) but not as adinoles, and that the grey and black slates (poor in iron) do not develop spots but are strongly adinolised.

Agrell (1939, 1941) provided a very detailed petrographic and mineralogical study, with some chemical analyses, of the adinoles from Dinas Head and reported tourmaline to be locally abundant. He also pointed out the similarity of mineralogical and chemical composition between adinoles

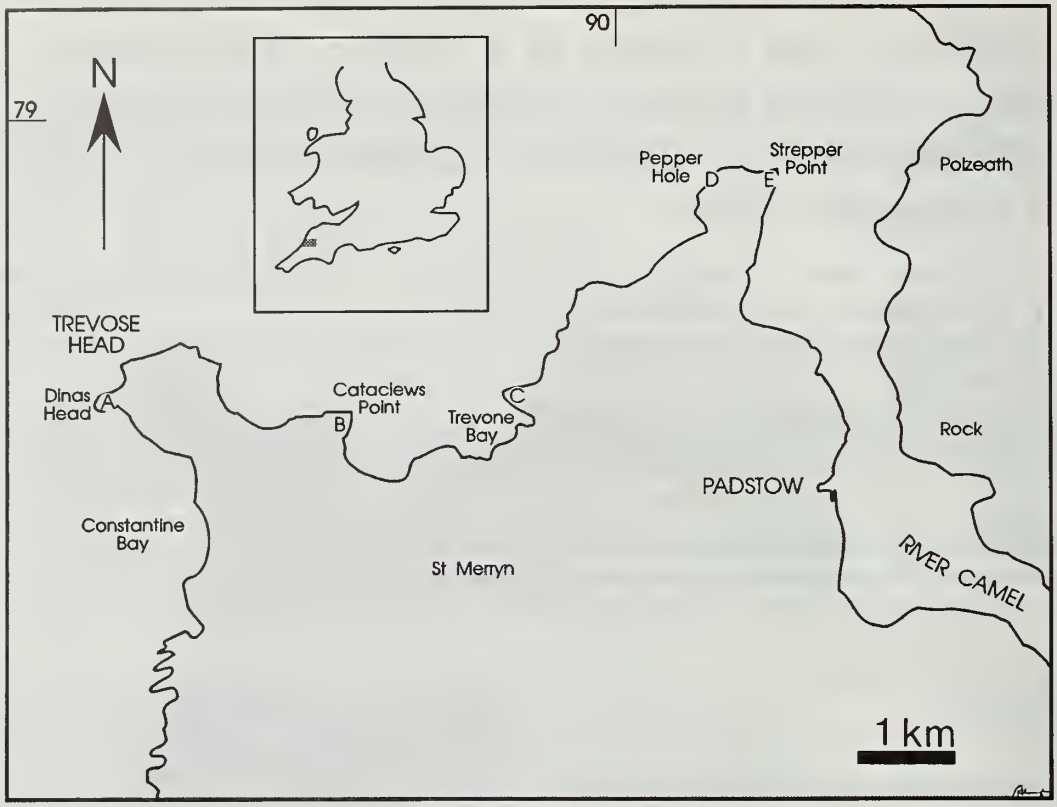

Fig. 1 Locality map of areas sampled. A = Dinas Head; B = Cataclews Point; C = Trevone Bay; D = Pepper Hole; E = Stepper Point.

and some keratophyric lavas and tuffs, and suggested that some rocks described as adinoles and of metasomatic origin are in reality tuffs altered by thermal metamorphism at the contact with basic intrusions. However, he concluded that the adinoles at Dinas Head were derived from a sediment, which had been metasomatised, and that the composition of the end-product adinoles is controlled by the metasomatic fluids emanating from the intrusive igneous dolerite rocks.

AIMS

From a systematic sampling of the adinoles, spilosites, slates and dolerites our aims were to: (1)Study the mobility and fixation of trace elements during the adinolisation process; (2)Investigate the formation of tourmaline (mobility and source of boron); (3)Compare the geochemistries of the dolerite and adinoles at Dinas Head with those of other similar rocks in the area; (4)Comment on the origin of adinoles.

In order to obtain representative samples for mineralogical and geochemical studies samples were collected from 3 measured sections of the Dinas Head rocks, the quarry section directly east of the headland and sites at Stepper Point, Pepper Hole, Trevone Bay and Cataclews Point (Figs 1 and 2). Details of the samples analysed are given in Table 1.

PETROLOGY AND MINERALOGY OF SAMPLES FROM DINAS HEAD

A comprehensive petrographic description of the rocks from Dinas Head was given by Agrell (1939), therefore the rocks studied here are only briefly described along with their mineral chemistries (below).

Dolerites

The massive intrusive units underlying the Dinas Head area and those studied from the Mackerel Cove, Stinking Cove and Quarry sections are albite-dolerites usually more than a metre thick with a mottled, dull dark-green surface. Below the High Water Mark (HWM), the dolerite has a weathered brown (limonitic) surface. At all localities it is extensively altered and little of the original mineralogy can be seen, but in less altered areas, ophitic textures can be recognised and some pyroxene is preserved. The areas of greatest alteration are marked by extensive chloritisation and carbonate development. The plagioclase feldspar (where unaltered) is albite (Ab_{90}) occurring as laths within the groundmass, and with pyroxene in ophitic texture. Light green chlorite with prussian blue interference colours, analyses in Table 2, often forms the matrix of the rock. An iron-rich carbonate occurs abundantly throughout the rocks, especially as small stringers. Ilmenite is common, mostly as skeletal plates and pyrite occurs in small amounts. Sample MC4 was collected close to

Table 1 Details of analysed samples.

Field No.	Lab. No.	Group No.	Details
MACKEREL COVE			
MC4	8466	2	Dolerite
MC5	8467	4	Sediment (carbonate-rich)
MC6	8468	4	Sediment (limestone)
MC7	8469	2	Dolerite
MC8	8470	4	Sediment (carbonate-rich)
MC9	8471	4	Sediment (carbonate-rich)
MC10	8574	1	Base of adinole (brown-spotted)
MC11	8575	1	0.3 m above MC10 (brown-spotted)
MC12	8472	1	6.0 m above MC10 (scarce brown spots)
MC13	8473	1	9.5 m above MC10 (green-spotted and banded)
MC15	8474	1	10.5 m above MC10 (massive adinole)
MC16	8475	1	17.0 m above MC10 (white massive adinole)
MC18	8476	1	24.0 m above MC10 (white, porcellaneous adinole)
MC21	8477	3	40.0 m above MC10 (white massive adinole)
MC22	8478	1	54.0 m above MC10 (white massive adinole)
MC23	8479	3	63.0 m above MC10 (white massive 'cherty' adinole)
STINKING COVE			
SC1a	8480	1	Spherulitic adinole
SC1b	8481	1	Spherulitic adinole
SC2	8482	4	Quartz-granite vein
SC3	8483	3	Adinole (2.0 m below SC1)
SC4	8571	4	Sediment (limestone)
SC5	8572	4	Sediment (carbonate-rich)
SC6	8484	1	Slate (fissile)
SC7	8573	4	Limestone band (2.0 m above faulted junction)
SC9	8485	2	Dolerite
SC10	8486	1	Adinole (1.0 m above adinole/dolerite contact)
SC11	8487	1	Adinole (20.0 m above adinole/dolerite contact)
SC14	8488	1	Adinole — brown-spotted (5.0 m above High Water Mark
SC15	8512	1	Adinole — brown-spotted (8.0 m above High Water Mark
SC16	8513	3	Adinole (due west of SC3)
SC17	8514	3	Adinole (directly below adinole/slate fault)
SC18	8489	3	Adinole (highest exposed outcrop)
SC19	8515	3	Adinole — green, massive (directly below adinole/slate fault
SC20a	8516	3	Adinole — green, massive (directly below adinole/slate fault
SC20b	8490	3	Adinole — black, massive (directly below adinole/slate fault
SC21	8517	3	Adinole (directly below adinole/slate fault)
47262	8502	3	From Agrell (1939), top of Stinking Cove
47263	8503	3	From Agrell (1939), top of Stinking Cove
47253	8504	3	From Agrell (1939), top of Stinking Cove
DINAS HEAD PROMONTORY			
DH1	8569	4	Dolerite?
DH4	8491	1	Adinole — brown, bedded (12.0 m above DH1)
DH5	8492	4	Adinole? — bedded (15.0 m above DH1)
DH6	8493	1	Adinole — grey, bedded (21.0 m above DH1)
DH7	8494	4	Shale — purple-grey with lozenges (26.0 m above DH1
DH9	8495	1	Adinole — white-weathered, massive (36.0 m above DH1
DH10	8570	2	Dolerite (47.0 m above DH1)
DH11	8518	1	Adinole (top of section, 56.0 m above DH1)
DINAS HEAD QUARRY			
DHQ3	8496	1	Adinole — grey-red, bedded
DHQ5	8566	1	Adinole — grey-red, slaty
DHQ6	8567	1	Adinole — brown-spotted
DHQ7	8497	1	Adinole — massive
DHQ8	8568	1	Adinole — white-weathered
DHQ9	8498	2	Dolerite — spotted
DHQ10	8499	1	Adinole
DHQ11	8500	4	Quartz vein
DHQ12	8501	2	Dolerite — altered
OTHERS			
PC5	8505	4	Sediment (Pepper Hole)
PC6	8506	2	Dolerite (Pepper Hole)
ST1	8673	4	Sediment (Stepper Point)
ST2	8674	2	Dolerite (Stepper Point)
ST5	8675	4	Slate (Stepper Point)
TR1	8676	2	Dolerite (Trevone Bay)
TR2	8677	4	Sediment (Trevone Bay)
TR3	8678	4	Slate — unaltered (Trevone Bay)
CAT2	8679	4	Sediment (Cataclews Point)
CAT3	8680	2	Dolerite (Cataclews Point)

Notes: Group 1 = sediments with Na_2O greater than 4.0%; Group 2 = dolerites; Group 3 = samples with boron greater than 400ppm; Group 4 = sediments with Na_2O less than 4.0%, and other samples

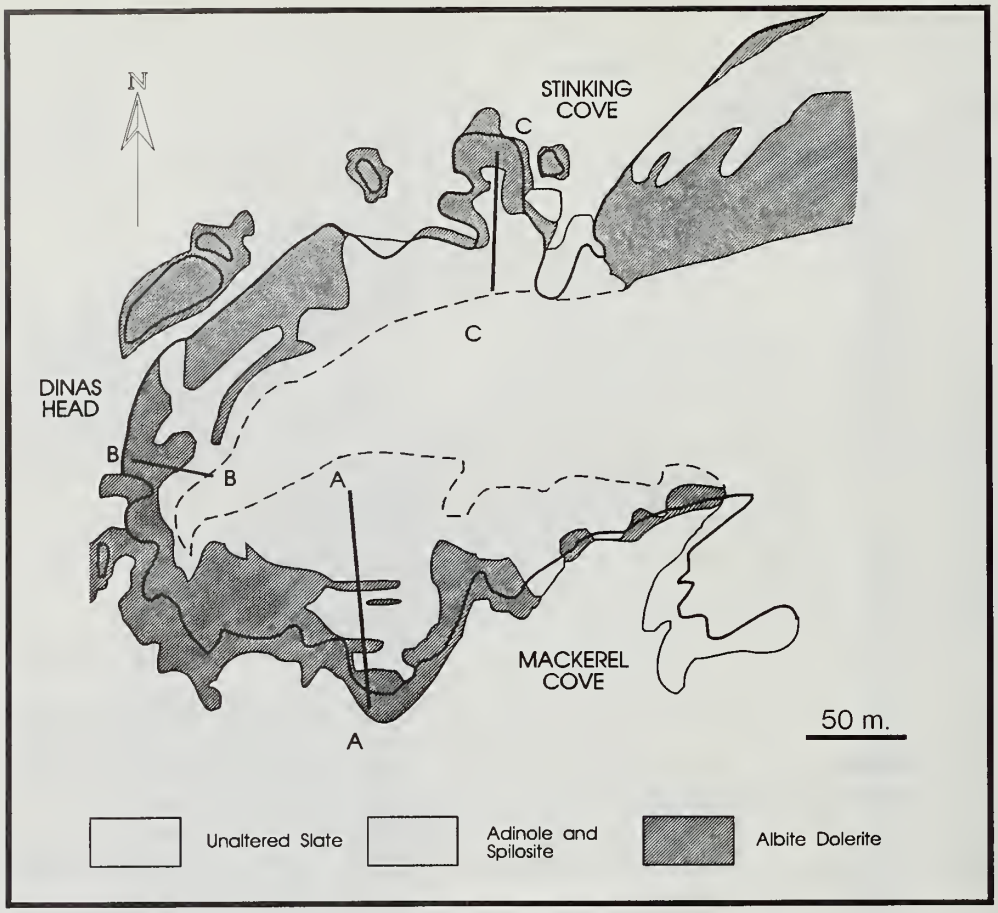

Fig. 2 Outline geological map (after Fox, 1895) of Dinas Head indicating locations of traverses A, B, and C for samples analysed.

the top of the dolerite intrusion at Mackerel Cove and consists of a mass of small euhedral albite crystals with chlorite, which may represent a chilled margin facies of the dolerite. The dolerite stringers (typically 25–50 cm thick) which cut the adinole sequence usually have been heavily carbonated and chloritised but original textures are better preserved with some remnant pyroxene. (Dolerite mineral analyses shown in Table 2, whole rock in Table 4).

Mackerel Cove section

The most complete sequence of adinole and spilosite development occurs above Mackerel Cove. A measured section was sampled from this area as shown in Fig. 2. Heights were recorded from the top of the massive dolerite intrusion found at HWM at intervals dependent upon change of rock lithology and texture.

The intrusive dolerite at the base of the section has an irregular surface from which smaller intrusions penetrate the sedimentary succession (Table 1). The beds of this sedimentary sequence dip between 20°–35° to the north and near the dolerite contact they are extensively quartz veined. The whole of this measured section was found to consist of various spilosite or adinole rocks. The distinctive white-weathering adinoles have a simple mineralogy of fine-grained albite and quartz, with minor chlorite, calcite and ankerite occasionally cut by thin carbonate-rich veins. Both calcite and ankerite are present as isolated, late-formed crystals or crystal patches. The carbonate-rich adinoles are often characterised by globular masses of ankerite up to 2 cm in diameter.

Above the extensive quartz veining is a somewhat irregular bed which is conglomeratic (or brecciated). Parts of this bed are extensively carbonated. Pebbles (?xenoliths) are albite-rich but much altered. This horizon is overlain by brown porcellaneous calcareous sediments, almost certainly originally limestone. These grade into a series of fine-grained, white and brown weathering rocks, containing extensive brown weathering (limonitic) iron oxides as spots and veins. Much of the iron oxide can be seen in thin section to be brown alteration products after pyrite. Above these beds, a major bluff is formed by rocks with distinct spotting and layering, these rocks have a very fine-grained matrix and are characterised by a random distribution of lozenge-shaped structures rimmed by iron carbonates. These beds are overlain by white-weathering rocks of a very fine grain size (albitic matrix) with dark diffuse spots of various sizes. None of the spots overprint original sulphide, most are diffuse pockets of albite and quartz with the original bedding often marked by black, filamentous material, probably graphite. Spots and veins rich in chlorite are also common in the rocks from this part of the section. Towards the top of the section spilosites comprising albite, quartz, chlorite, and filamentous carbon-

Table 2 Typical microprobe analyses of minerals from dolerites.

	MC2 Albite	MC2 Chlorite	MC4 Albite	MC4 Chlorite	MC7 Albite	MC7 Chlorite	DH2 Albite	DH10 Albite	DH10 Chlorite	DHQ9 Albite	DHQ9 Chlorite	ST2 Albite	ST2 Chlorite	TR1 Albite	TR1 Clino-pyroxene	TR1 Amphi-bole
	1	2	3	4	5	6	7	8	9	10	11	12	13	14	15	16
SiO2	66.80	25.10	66.73	27.03	67.77	26.22	67.78	67.29	28.20	65.00	27.49	65.64	28.18	66.44	47.50	39.57
TiO2	<.05	<.05	<.05	<.05	<.05	0.09	<.05	<.05	2.78	<.05	0.09	0.00	<.05	<.05	2.04	4.89
Al2O3	20.20	20.48	20.09	19.12	19.26	20.05	19.61	19.86	17.31	21.56	17.99	20.59	16.54	20.26	5.46	11.94
FeO	0.53	28.81	0.26	29.59	0.19	25.08	0.80	1.09	21.83	0.40	26.57	0.56	25.94	0.30	6.28	13.66
MnO	<.05	0.11	<.05	0.11	<.05	0.20	<.05	<.05	0.06	<.05	0.07	<.05	0.07	<.05	0.17	0.18
MgO	<.05	10.59	<.05	10.70	<.05	13.21	<.05	<.05	15.81	<.05	13.50	<.05	15.39	<.05	13.14	10.80
CaO	0.61	0.13	0.51	0.21	0.13	0.09	0.14	0.15	0.00	1.82	0.17	0.82	0.19	0.25	22.83	11.67
K2O	0.22	0.15	0.24	0.08	0.03	0.10	0.72	0.03	0.19	0.14	0.08	0.47	0.15	0.54	<.02	0.99
Na2O	11.60	0.22	11.29	0.64	11.99	0.49	10.37	11.63	0.17	10.92	0.34	10.41	0.38	10.47	0.55	2.96
TOTAL	99.96	85.59	99.12	87.48	99.37	85.53	99.42	100.05	86.35	99.84	86.30	98.49	86.84	98.26	97.97	96.66
Ab	96.0		96.3		99.2		95.0	99.1		90.8		93.2		95.5		
An	2.8		2.4		0.6		0.7	0.7		8.3		4.1		1.3		
Or	1.2		1.3		0.2		4.3	0.2		0.9		2.7		3.2		

Analyses 1–6. Mackerel Cove section.
Analyses 7–9. Dinas Head section
Analyses 10–11. Dinas Head Quarry section.
Analyses 12–13. Stepper Point
Analyses 14–16. Trevone Bay.
Analyses made by energy-dispersive microprobe.

aceous material predominate. There are also calcite-rich spots, with the calcite present either as single crystals or as clusters. At the top of the section, the rocks are a mixture of spilosites and adinoles, with coarse- to fine-grained albite, aggregates of leucoxene (after anatase) and quartz veining. Microprobe analyses of albite and chlorite from several samples are given in Table 3. Chemical analyses of two samples, MC21 and MC23 (Table 4), showed them to be boron-rich.

Stinking Cove section

The Stinking Cove section (Fig. 2) is extensively faulted and a complete succession cannot be traced. However, the section is of importance in that it contains excellent examples of polygonal (spherulitic) adinole development, and areas of high boron content, as ascertained by chemical analysis.

On a rock shelf above the dolerite contact and above the HWM is a spectacular development of spherulitic and polygonal adinole, not seen elsewhere on Dinas Head. These rocks grade above and below into apparently normal adinoles. However, chemical analyses and scanning electron microscopy indicate that some of these rocks are K-rich, and that white mica (probably sericite, e.g. Fig. 3b) predominates over albite. Much of this area is ribbed by thin veins of carbonate and the faulted western margin is marked by coarse quartz veining carrying lead mineralisation (SC2, Table 4). To the south, the adinoles are cut out by a fault and the resultant low cliff section comprises unaltered slates and massive limestone bands. These rocks do not show evidence of adinolisation or spilositisation. The rocks above and below the polygonal development show, on analysis, the patchy development of high boron-rich areas (e.g. SEM photo, Figs 3c, 3d), which is consistent with Agrell's (1939) report of colourless dravite in the rocks, although the matrix is often sericite-rich, not albite-rich.

In this section, the rocks are typically composed of a fine-grained groundmass of albite, and/or sericite, containing small spots with opaque centres. Some of the spots are carbonate and/or chlorite-rich. Small skeletal ilmenite grains are common and in places appear to pick out original bedding in the rocks. At x100 magnification the groundmass of the boron-rich rocks is indistinguishable from that of boron-poor rocks, except that they consist almost entirely of a mat of small albite laths and show very little spot development or carbonatisation (e.g. SEM photo, Fig. 3a).

The polygonal adinole consists of a fine-grained skeletal framework forming irregular 5–10 mm sided polygons, the whole structure consisting of a groundmass of albite, quartz and chlorite. Original bedding can be recognised and Agrell (1939) has proposed that these adinoles be divided into different types because the albite in some parts is coarser and forms a (crude) spherulitic texture. The edges of both the polygonal and spherulitic types tend to stand out as weathered surfaces. Ankerite occurs both as ribs between some of the polygons, and as individual rhombs. Small black filamentous (carbonaceous) stringers were seen in some of the thin sections studied and thin quartz veins cut all types of structure.

Closer to the dolerite contact, within an unfaulted part of the sequence, a series of spotted rocks similar to those described from elsewhere on Dinas Head and Stepper Point is exposed. These spotted rocks contain larger, often diffuse carbonate-rich spots or structures, which often appear to be aligned along bedding. The groundmass consists of fine-grained albite and chlorite, and small skeletal ilmenite grains and sulphide blebs. The centres of the larger carbonate-rich spots are often cavernous and many have a rim accentuated by colouration due to brown limonite after ankerite.

Within a faulted block of this rock succession, closest to the contact with the massive dolerites, spilosites are abundantly developed. These rocks, with a matrix of albite and feather-

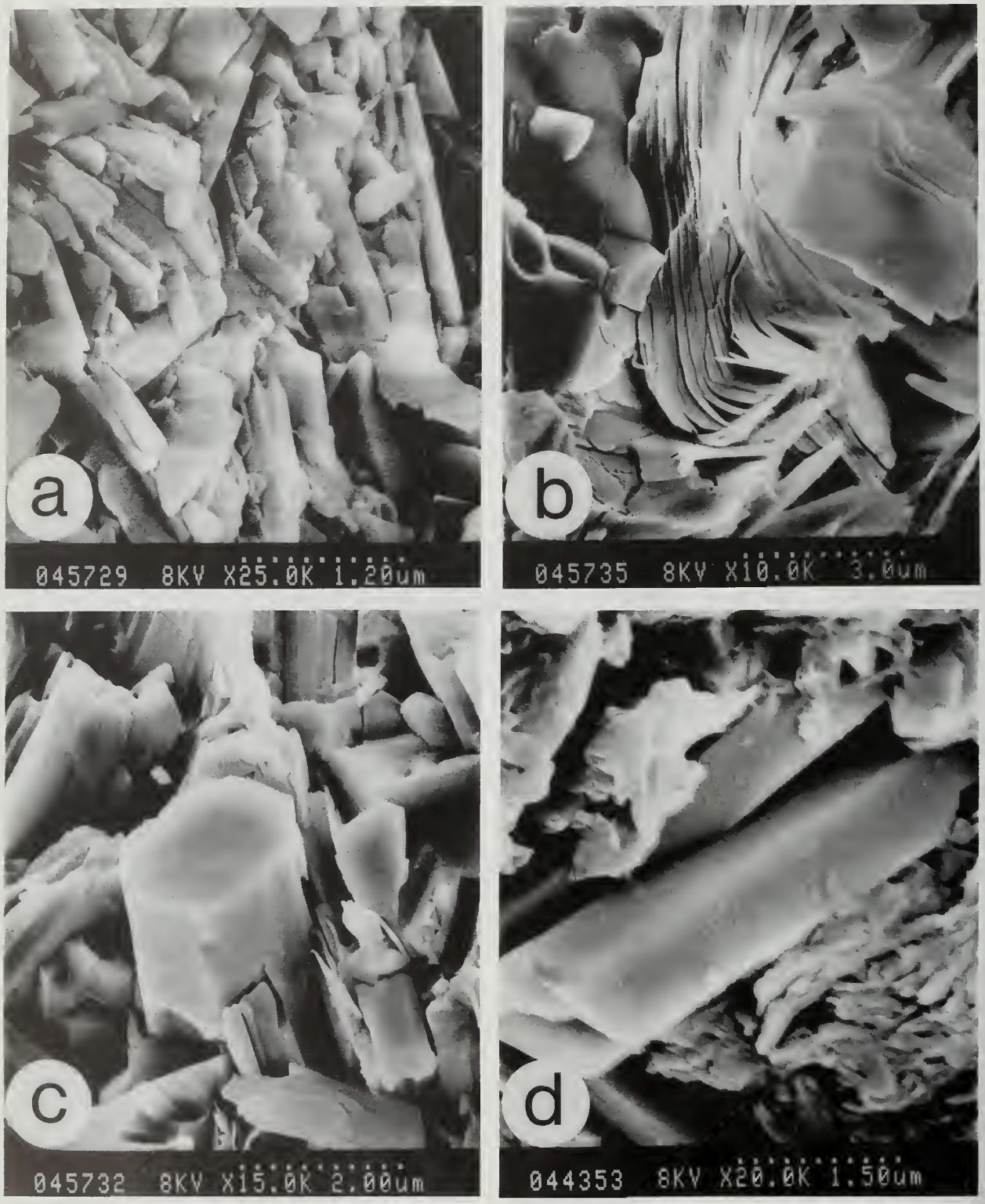

Fig. 3 Scanning electron micrographs of selected samples. 3a = SC19 albite; 3b = SC3, sericite; 3c = SC3, quartz + dravite; 3d = SC18, dravite + sericite.

ing stringers of chlorite, are rather different from the typical rocks seen in other sections.

Dinas Head section

The measured section at the western extremity of Dinas Head (Fig. 2) is a succession of spilosites and adinoles interdigitating with thin dolerite intrusions above massive weathered dolerite. The top of the massive dolerites is extensively sheared and veined with quartz.

Like the sections at Stinking Cove and Mackerel Cove, the sequence at Dinas Head is a series of spilosites and adinoles with different textures. Predominant is a grey weathering, fine-grained bedded sequence with brown ankeritic rich spots. Another common feature of the rocks in this section is the prevalence of patches of chloritic alteration. Recognisable in hand specimen, these patches show no definable or constant shape, and often consist of a central core of calcite rhombs enclosing ilmenite grains. Altered sulphide grains (mostly pyrite) impart brown spotting to weathered surfaces. These rocks grade into fine-grained albite-rich rocks, which display remnants of the original bedding (emphasised by carbonaceous filaments). They are also characterised by small calcite patches, spots and frequent limonite-lined calcite veining.

Some 25 m above the top of the dolerite there is a good example of the limonite-rich, 'lozenge' textured rocks, similar to those described from the Stepper Point locality. These rocks have a fine-grained albitic matrix, with carbonaceous filaments and substantial thin veining, most of which is chlorite-rich. Here the lozenge structures, essentially comprising calcite and lined with brown iron oxides, must be formed late because they cut both the chlorite veins and carbonaceous filaments. These rocks grade into massive bedded units of spilositic texture. The top of this section is marked by banded, white-weathering adinoles with a matrix of albite and chlorite. Sericite-rich rocks were not observed here.

Quarry section

The section exposed in the quarry at the eastern end of the Dinas Head promontory has been extensively folded and faulted, such that the relationships between individual parts cannot be traced. The section consists of a repeatedly sheared sequence of black and purple slates (shales). Although the section is intruded by massive dolerite units to the south, most of the shales do not appear to have been altered and are similar to the beds at the top of the Stinking Cove section. However, toward the centre of the section, between two convergent shear zones, some spotted rocks have been developed. These rocks have a fine-grained albitic matrix. The spots are dark, intense in appearance, and often preferentially aligned. Lozenge shaped structures, such as those found at Dinas Head, also occur.

The dolerite in the quarry section is medium-grained but very altered, and in places has a 'spotted' surface appearance.

OTHER AREAS OF STUDY

The succession of rocks from Dinas Head, described as adinoles, is very much thicker (approximately 60 m) than other recorded adinole sequences, especially in comparison with potentially similar rocks directly associated with intrusive dolerite complexes in the same province of Cornwall. Dolerites are exposed along the coastal sections from Dinas Head eastwards to Stepper Point, where the associated sediments close to the contacts with the dolerite are often characteristically fine-grained, white-weathering with carbonate 'spot' and vein growth (cf. Dinas Head — Stepper Point occurrences). Samples of both dolerite and contact country rock have been sampled and analysed for comparison with those at Dinas Head (Tables 1 and 4). A brief field and petrological description of these rocks is given below.

Table 3 Typical microprobe analyses of minerals from adinoles and spilosites.

	MC10 Albite	MC12 Albite	MC13 Albite	MC13 Chlorite	MC14 Albite	MC14 Chlorite	MC15 Albite	MC15 Chlorite	MC23 Albite	MC24 Albite	SC1 Albite	SC10 Albite	SC14 Albite	ST1	TR2	PC5
	1	2	3	4	5	6	7	8	9	10	11	12	13	14	15	16
SiO2	67.86	68.88	66.65	25.51	67.29	24.79	67.79	26.14	67.69	67.82	67.19	68.46	67.1	58.45	55.32	64.67
TiO2	0.07	0.08	<.05	<.05	<.05	0.05	<.05	<.05	0.12	<.05	<.05	0.07	0.15	<.05	0.43	<.05
Al2O3	19.08	19.01	19.34	21.65	18.83	21.2	18.84	21.04	19.11	19.12	19.7	18.89	19.06	22.00	24.14	19.23
FeO	<.05	<.05	0.12	28.61	1.25	28.8	0.22	29.81	0.14	0.4	0.15	0.11	0.1	2.37	1.43	5.72
MnO	0.11	<.05	<.05	<.05	<.05	0.17	<.05	0.13	<.05	<.05	<.05	<.05	<.05	<.05	0.15	<.05
MgO	<.05	<.05	<.05	9.41	0.13	9.27	<.05	7.78	<.05	<.05	<.05	<.05	<.05	1.34	1.09	2.78
CaO	0.15	0.06	0.21	0.17	0.05	0.05	0.12	0.17	0.04	0.08	0.1	0.1	0.15	0.27	0.1	<.05
K2O	0.11	0.08	0.03	0.12	0.09	0.12	0.01	0.1	0.11	0.22	0.34	0.24	0.04	6.84	7.3	4.14
Na2O	10.90	10.67	11.28	0.37	10.47	0.18	10.83	0.52	10.99	10.69	11.1	10.14	11.02	0.09	0.18	<.05
TOTAL	98.28	98.78	97.63	85.84	98.11	84.63	97.81	85.69	98.2	98.33	98.58	98.01	97.62	91.36	90.14	96.54
Ab	98.6	99.2	98.8		99.2		99.3		99.2	98.3	97.5	98.0	99.0			
An	0.8	0.3	1.0		0.2		0.6		0.2	0.4	0.5	0.5	0.7			
Or	0.6	0.5	0.2		0.6		0.1		0.6	1.3	2.0	1.5	0.3			

Analyses 1–10. Mackerel Cove section, adinole and spilosite.
Analyses 11–13. Stinking Cove section
Analysis 14. Stepper Point
Analysis 15. Trevone Bay
Analysis 16. Pepper Hole

Stepper Point (GR SW 916,785)

The best exposures of the dolerite-sediment contacts outside the Dinas Head area are at Stepper Point. Here, thick dolerite intrusions have been extensively quarried and relatively fresh sections can be sampled. Within the southern section of these quarries the contact between the dolerite and the country rocks is well exposed. Although the country rocks vary from grey to green to purple slates, the rocks adjacent to the contact are spotted spilosites, with small, dark grey, diffuse spots. The more diffuse spots often contain minute black areas, which are not sulphide or limonite-rich and may be original carbonaceous material. A characteristic feature of these rocks is that within a metre of the contact, ferruginous, calcareous nodules are developed, the cores of which are often weathered out and slightly elongated along bedding. Further from the contact, the country rock sequence of grey/green/purple slates prevails.

Specimens of dolerite were sampled from the centre of the intrusion in the main quarry and also from close to the contact. Although the hand specimens appeared relatively fresh, thin section examination revealed all samples as being extensively altered. Electron microprobe analyses and whole rock chemical analyses are shown in Tables 2 and 4. In hand specimen the dolerites are a dull, grey-green colour and essentially non-porphyritic. Thin sections show characteristic clots of intergrown feldspars (albite Ab_{93} — see Table 2), which are occasionally clear, but usually sericitised. The pyroxene, originally augite, has been extensively altered to chlorite and a dark brown product of variable compositions; ophitic textures can still be recognised. Large ilmenite masses and copious euhedral apatites are common in all the thin sections studied.

Thin section examination of those rocks directly above the contact, showed that they are spilositic in texture, very fine grained and often have a calcareous matrix. The rock is distinctly spotted, often with minute dark spots which appear to be formed from remnant organic material. Within 25 cm of the contact, these fine-grained spilosites merge into similar fine-grained rocks with distinct lozenge-shaped ferruginous, calcareous structures. The matrix of these rocks is consistently of a sericitic composition.

Pepper Hole (GR SW 907,782)

Samples of dolerite and associated purplish-grey slates were collected from a cliff section above the main dolerite intrusion. Here the dolerites occur as thin sills, up to 10 cm thick, being stringers from the massive dolerite intrusion cutting through the succession of purple-red-grey slates. The argillaceous rocks consist of a matrix of very fine-grained sericite incorporating about 10% quartz and feldspar fragments. The rocks are cut by minor limonite-stained calcite veins. No preferred orientation was observed to the fabric of these rocks, and, although they do contain many altered limonitic blebs, they do not have the typical spilositic (or adinole) texture or composition. This indicates a very low level of alteration by the associated minor dolerite intrusions. The medium-grained dolerite is considerably altered — pyroxene to chlorite and feldspar to sericite — but remnant ophitic texture is present. Apatite and ilmenite are common in the groundmass.

Trevone Bay (GR SW 889,764)

To the north of Trevone Bay and immediately west of the eroded 'blow-hole' shown on the O.S. map as Round Hole, a massive dolerite intrusion cuts through sediments comprising alternating bands of slates and limestones.

The non-porphyritic dolerite has mostly a weathered limonitic surface and is in contact with a series of mainly bleached, poorly spotted slates (spilosites). These are extensively veined by both quartz and calcite. Although in hand specimens the dolerite appears extensively weathered, thin section examination shows it is less altered than dolerites from other localities sampled in this study. However, it does contain considerable interstitial calcite. The dolerite is rich in augitic pyroxene, brown hornblende, chlorite and laths of albitic plagioclase feldspar. Although pyroxenes are often altered to amphibole there is only minor alteration of the amphibole to chlorite. Apatite and ilmenite are common as euhedral crystals, and calcite occurs interstitially. Typical analyses of the major phases are shown in Table 2.

The dolerite intrusion appears to have altered the surrounding sediments to typical spilosites, characterised by small dark grey-black spots, these sometimes associated with small pyrite crystals which are often altered to limonitic pseudomorphs. The fine grained matrix and diffuse spots are sericitic in composition (Table 3). Whole rock analyses of dolerite and spilosite are given in Table 4.

Cataclews Point (GR SW 873,762)

At Cataclews Point massive dolerite sills cut a succession of slates, some interbedded limestones and cherts. The shales (slates) in close contact with, or engulfed by the dolerites are bleached and have a typical spilositic texture. This section has been extensively sheared and parts of the sequence have been described as cataclasites (Fox, 1895). Samples were collected from the less tectonised areas where igneous-sedimentary contacts could be recognised. Even so the coarse-grained dolerites in thin sections were found to be extensively altered with almost complete sericitisation of the feldspars and chloritisation of mafic phases. Where clear (unaltered) feldspar laths were analysed, the composition is varied, but not albitic. Very little original pyroxene remained, but textures suggest replacement by both green and brown amphibole, the latter being a Ti-rich variety. Pyrite and ilmenite are both present in the rock.

The associated sedimentary rocks have a very fine grained sericitic matrix and conspicuous spotting, often with a slight elongation of the spots. These rocks have abundant, small spots of a similar size; spots and matrix are generally of a similar sericitic composition although the spots are relatively iron rich. Whole rock analyses are given in Table 4.

ANALYTICAL METHODS

The specimens collected were crushed in a jaw crusher and comminuted to a particle size of $\not> 180\mu m$ by grinding in agate. All powders were dried at 110°C prior to sampling for analysis. Deionised water and analytical grade reagents (or better) were used throughout the various preparation procedures.

Major and minor elements

Approximately 100 mg of powder, accurately weighed, was mixed with 500±1 mg of lithium metaborate flux in a platinum/5% gold crucible and fused at 950°C until a transparent melt was obtained. The hot fusion bead was quenched in 140 ml of dilute nitric acid (1M), contained in a plastic beaker, and the mixture was stirred at ambient temperature until the solid dissolved. The clear solution was washed into a 250 ml volumetric flask and made to volume with water.

Analyses of the prepared solutions for Si, Ti, Al, total Fe, Mn, Mg, Ca, Na and K were made by inductively-coupled plasma (ICP) emission spectrometry using a Fison's ARL 3410 Minitorch machine. The instrument parameters were adjusted according to the manufacturer's recommendations and the system was calibrated with a series of multi-element synthetic standards prepared from commercial, spectroscopically pure, stock solutions. Appropriate corrections were made to compensate for background emission and instrumental drift. Several international standard reference rocks were processed as unknown samples in order to verify the accuracy of the procedure.

Combined water and total carbon, expressed as CO_2 were determined in accurately weighed sample aliquots of approximately 25 mg following the procedure described by Din and Jones (1978). Ferrous iron was estimated volumetrically by titration with standardised potassium permanganate, a variation of the method described by French and Adams (1972).

Trace elements

Up to 27 trace elements were determined by instrumental neutron activation analysis (INAA) and ICP. Not all of the elements listed below were determined in all samples.

Solutions for the determination by ICP of Ba, Be, Cu, Li, Nb, Ni, Pb, Sr, V, Y, Zn and Zr were prepared using a standard perchloric-hydrofluoric acid procedure to dissolve 1 g of rock in a final solution volume of 50 ml.

INAA data for selected rare earth elements (REE), As, Cr, Co, Cs, Hf, Rb, Sb, Sc, Ta, Th and U were obtained from 100 mg of rock powder following the technique described by Williams and Wall (1991).

Boron

Boron was measured quantitatively by ICP in the aqueous leachates (25 ml) prepared from a fused mixture of sodium carbonate (500±1 mg) and about 50 mg of accurately weighed sample powder. Sulphur and phosphorus were measured in the same solutions.

Qualitative maps of the boron distribution in thin sections of selected samples were made, using the solid state nuclear track detection technique, according to the procedure described by Din and Henderson (1982).

Data for boron isotope studies were obtained by ICP mass spectrometry, using equipment at the British Geological Survey Laboratories, Gray's Inn Road, London WC1. Solutions of the samples, together with a National Bureau of Standards isotopic reference (SRM951), were prepared from the powdered materials after fusing with 1000±30 mg of potassium hydroxide in vitreous carbon crucibles and leaching and dissolving in 50 ml dilute nitric acid (1M). These solutions were made up to 200 ml and tenfold dilutions were prepared for ICPMS. Sample weights were chosen to yield solutions containing <5 ppm boron on dilution.

GEOCHEMISTRY

Dolerites

At Dinas Head, dolerite is seen in three localities — at Mackerel Cove and Stinking Cove, where it forms the base of the promontory (Fig. 1), and in the quarry section to the east. At Mackerel Cove, and to a lesser extent at Stinking Cove, the dolerite often occurs interfingered with the associated adinoles although actual contacts were not observed. In the field, the dolerite appears evenly medium-grained and relatively fresh at the promontory, but is more altered in the quarry section, and in places has a 'spotty' appearance.

Six samples of the dolerite were selected for chemical analysis — two from the Mackerel Cove section, one from Stinking Cove, one from Dinas Head and two from the quarry section. The results (Table 4), show many similarities for all samples, and particularly for those elements considered to be less mobile during alteration processes, i.e. the REE, Hf, Ta and Th, indicating that the dolerite is likely to be a single intrusion. The overall chemical composition of the dolerite is similar to that of other Upper Palaeozoic tholeiitic basalts from south-western England (Floyd 1982).

Dolerites from four other localities in N. Cornwall, reported to be associated with adinoles, were also sampled and analysed. These were from Pepper Hole, Stepper Point, Trevone Bay and Cataclews Point: data are given in Table 4. From a comparison of these data with those from Dinas Head, Table 4, and associated diagrams (Fig. 4), it is clear that for many elements significant differences exist between the dolerite from Dinas Head and those from Pepper Hole and Trevose Head, and minor differences between Dinas Head dolerites and those from Stepper Point. There is however a strong similarity between the dolerites from Dinas Head and those from Cataclews Point; compare for example data for elements Sc, Co, Ta, Th, U and REE, Table 4.

Sediments

A total of 54 sediments were selected for whole rock geochemistry, 49 of those from the four sampled sections of the Dinas Head area. The remaining sediments analysed were those associated with the dolerites from Stepper Point, Pepper Hole, Trevone Bay and Cataclews Point.

Sediments from the Dinas Head sections are plotted on the $(Na_2O.Al_2O_3) - (K_2O.Al_2O_3) - (Fe_2O_3 + FeO + MgO + MnO + CaO)$ ternary diagram (Fig. 5) following Agrell (1939), in order to ascertain which sediments plot in the 'adinole', 'spilosite + desmosite' and 'slate' fields. There is a relatively good correlation with Na_2O% and little overlap within the discriminated fields. Those plotting in the 'adinole' field have Na_2O contents ranging from 6.22% (MC10) to 11.10% (SC11), those in the 'spilosite + desmosite' field range from 1.64% (47263) to 7.35% (MC13) and those in the 'slate' field have Na_2O contents <1.64%.

From this diagram also, it can be seen there is a complete gradation from Na_2O-rich, K_2O-poor sediments (e.g. MC11, Na_2O = 9.86%; K_2O = 0.20%) in the 'adinole' field, to Na_2O-poor, K_2O-rich sediments (e.g. SC20A, Na_2O = 0.51%; K_2O = 4.56%) in the 'slate' field. In the 'adinole'

Table 4 Chemical analyses of whole rock samples.

SAMPLE	MC4	MC5	MC6	MC7	MC8	MC9	MC10	MC11	MC12	MC13	MC15	MC16	MC18	MC21	MC22	MC23	SC1A
SiO_2	46.3	50.2	9.50	50.8	47.5	47.6	70.9	68.7	63.5	55.8	57.2	69.4	66.6	70.3	71.0	66.1	63.0
TiO_2	1.71	0.41	0.01	1.61	1.30	1.16	0.61	0.65	0.61	0.82	0.69	0.50	0.68	0.69	0.58	0.68	0.55
Al_2O_3	15.8	8.10	1.37	16.3	15.6	14.9	12.8	16.7	16.6	20.0	19.1	13.6	18.6	17.2	16.7	19.8	17.2
Fe_2O_3	1.23	0.03	0.82	1.29	0.56	0.37	1.89	0.67	0.80	2.39	1.06	0.88	0.14	0.42	0.05	0.00	0.20
FeO	8.43	5.43	11.1	8.56	7.02	6.40	0.15	0.10	1.17	5.88	7.89	4.06	0.79	0.34	0.45	0.51	0.61
MnO	0.12	0.21	0.34	0.09	0.11	0.09	0.08	0.03	0.06	0.03	0.03	0.05	0.03	0.02	0.02	0.02	0.06
MgO	4.09	4.29	8.72	5.46	5.76	6.95	0.28	0.05	1.28	2.48	2.30	1.70	0.53	0.62	0.36	1.05	0.72
CaO	6.25	11.2	27.3	2.91	5.39	5.39	2.75	0.38	3.28	0.20	0.16	1.20	0.70	0.09	0.08	0.15	3.91
Na_2O	4.38	1.11	0.14	4.70	2.35	2.53	6.22	9.86	8.15	7.35	7.03	5.43	10.40	8.60	9.17	8.35	8.58
K_2O	0.83	1.46	0.21	0.47	1.90	1.52	0.67	0.20	0.22	0.43	0.26	0.15	0.18	0.10	0.08	0.25	0.30
P_2O_5	0.19	0.09	0.03	0.09	0.15	0.11	0.20	0.26	0.09	0.20	0.16	0.07	0.09	0.05	0.08	0.14	0.03
H_2O^+	3.84	1.43	0.48	4.08	4.01	4.23	1.02	0.32	0.87	3.03	3.14	2.06	0.58	0.51	0.44	0.68	0.69
CO_2	5.35	16.2	37.9	3.66	7.54	7.59	2.65	0.31	3.51	0.15	0.07	1.10	0.60	0.22	0.13	0.20	3.01
others	0.43	0.27	0.14	0.41	0.26	0.29	0.14	0.07	0.12	0.98	0.32	0.22	0.12	0.91	0.12	1.44	0.21
O=S	–0.09	–0.05	–0.00	–0.10	–0.01	–0.01	–0.01	0.00	–0.00	–0.38	–0.07	–0.05	–0.00	–0.01	–0.01	–0.01	–0.01
TOTAL	98.9	100.3	98.0	100.3	99.4	99.1	100.3	98.3	100.3	99.4	99.3	100.4	100.0	100.1	99.2	99.4	99.1
$Fe_2O_3(T)$	10.6	6.06	13.1	10.8	8.36	7.48	2.06	0.78	2.10	8.92	9.83	5.39	1.02	0.80	0.55	0.44	0.88
S	1900	1100	80	2000	200	200	200	<50	90	7600	1500	1000	50	200	200	300	200
Be	1.7	1.4	0.8	1.3	1.8	2.1	0.8	0.6	1.1	1.4	1.6	1.0	0.9	0.9	0.7	1.9	1.0
Li	123	38	9	129	118	155	27	5	27	141	131	88	17	7	13	2	14
B	<25	40	<25	<25	40	40	25	<25	<25	<25	<25	<25	<25	2500	<25	4100	80
Sc	34.2	13.5	9.1	32.2	26.2	26.6	15.2	9.7	13.9	18.2	18.0	8.5	15.2	17.9	10.4	14.7	12.3
V	245	125	66	234	191	199	110	54	83	180	158	83	119	97	90	123	102
Cr	222	85	12	324	243	339	104	72	85	117	103	77	90	104	82	116	148
Co	33.0	12.0	6.3	40.0	32.3	29.6	2.6	0.5	5.0	37.7	23.9	23.6	13.8	2.7	1.5	0.9	1.5
Ni	20	43	21	64	105	171	25	10	40	102	163	82	117	29	71	nf	63
Cu	31	19	23	17	19	20	8	5	22	40	20	37	6	5	5	8	34
Zn	57	24	21	49	63	42	61	10	44	44	26	34	19	9	8	20	307
As	20	19	1	24	42	50	24	6	6	63	19	28	1	7	3	2	nf
Rb	47	81	21	20	140	83	33	5	60	60	65	65	40	50	50	50	30
Sr	603	352	726	201	232	340	160	147	155	126	92	88	122	89	116	98	228
Y	22	21	31	18	20	17	19	17	16	20	14	12	10	5	24	10	34
Zr	88	47	22	72	110	75	102	107	95	130	120	92	108	100	80	100	100
Nb	11	7	9	11	10	12	9	11	10	9	8	7	15	15	11	1	16
Sb	6.4	2.6	0.6	2.8	3.4	4.5	6.2	3.8	1.9	1.6	nf	1.8	1.0	1.6	0.7	1.1	1.3
Cs	7.0	5.3	1.7	2.1	7.9	8.8	2.3	0.7	1.1	1.2	1.2	0.8	0.6	0.5	0.7	0.7	0.9
Ba	112	95	16	60	118	129	66	23	27	37	28	15	23	17	18	30	30
La	7.5	15.9	5.1	13.3	17.8	27.2	11.4	14.0	21.4	95.0	33.5	21.6	38.8	9.5	20.7	3.3	5.8
Ce	17.9	26.6	13.0	29.5	30.3	45.8	21.0	22.5	58.3	180.0	59.8	47.1	65.8	21.5	62.0	5.8	15.5
Nd	12.8	13.8	11.5	15.7	16.7	22.4	11.0	9.5	33.8	80.2	21.2	26.4	22.2	8.3	39.8	4.6	8.4
Sm	3.28	3.38	4.12	3.47	3.94	3.92	2.28	2.18	6.38	12.20	4.79	4.52	3.64	1.67	5.46	1.45	2.19
Eu	1.59	1.36	2.86	1.02	1.10	0.85	0.63	0.46	0.98	2.36	0.99	0.95	0.55	0.33	0.48	0.23	0.52
Gd	4.6	2.7	5.2	3.3	3.9	2.8	2.9	3.3	5.3	10.5	5.4	3.6	2.8	1.5	5.5	1.5	4.3
Tb	0.71	0.57	0.89	nf	0.76	0.60	0.45	0.35	0.67	1.78	0.71	0.50	0.40	0.18	0.96	0.25	0.74
Tm	0.27	0.26	0.41	0.32	0.45	0.36	0.24	0.22	nf	0.85	0.39	0.30	0.27	0.11	0.52	0.00	0.66
Yb	2.10	1.41	1.64	1.85	2.24	1.80	2.05	1.90	1.89	5.65	2.22	1.82	1.15	0.66	2.91	1.38	3.23
Lu	0.27	0.21	0.21	0.26	0.32	0.24	0.29	0.28	0.23	0.74	0.22	0.24	0.16	0.12	0.36	0.19	0.47
Hf	2.2	0.9	0.2	2.3	2.8	2.0	2.5	2.7	2.7	4.0	3.4	2.0	3.2	3.1	2.7	3.2	3.0
Ta	0.48	0.22	0.05	0.51	0.49	0.35	0.81	0.92	0.80	1.23	1.00	0.67	0.98	0.94	0.87	1.00	0.92
Th	0.65	1.90	0.20	0.70	0.83	1.20	7.00	8.40	8.30	18.60	9.20	7.30	7.30	8.00	8.60	10.00	10.10
U	0.2	0.5	0.2	0.3	0.7	0.9	2.4	1.4	1.2	2.9	2.2	1.5	1.6	1.8	2.1	2.5	2.4
Pb	24	28	51	48	38	50	16.7	19.8	7	20	14	17	15	13	8	27	47

Table 4 *contd.*

SAMPLE	SC1B	SC2	SC3	SC4	SC5	SC6	SC7	SC9	SC10	SC11	SC14	SC15	SC16	SC17	SC18	SC19	SC20A
SiO_2	58.8	87.1	47.8	4.09	30.5	59.4	0.34	41.4	60.7	63.4		65.0	66.5	47.0	38.0	76.7	68.3
TiO_2	0.50	0.09	1.25	0.03	0.03	0.87	nf	1.33	0.70	0.75		0.61	0.66	1.41	1.37	0.50	0.89
Al_2O_3	16.3	1.32	28.4	0.41	0.71	21.9	0.02	14.4	17.9	18.5		17.2	18.8	32.7	35.8	13.9	21.7
Fe_2O_3	0.43	0.22	0.00	1.22	11.90	1.81	0.08	1.00	0.30	0.07		0.16	0.13	0.23	0.62	0.20	0.31
FeO	1.19	1.88	1.81	0.58	0.24	3.81	0.47	8.71	0.47	0.20		0.43	0.10	0.14	0.71	0.32	0.08
MnO	0.10	0.03	0.03	0.36	0.55	0.04	0.14	0.16	0.07	0.05		0.02	0.01	0.01	0.02	0.01	0.01
MgO	1.28	0.60	6.00	0.22	0.60	1.77	0.32	8.11	1.10	0.40		1.64	0.69	2.38	6.54	1.91	0.58
CaO	6.07	0.01	1.47	53.3	28.4	0.03	55.7	7.18	4.65	2.20		2.49	0.85	0.33	0.54	0.45	0.08
Na_2O	7.67	0.23	1.50	0.10	0.17	0.59	0.03	1.55	8.63	11.10		6.81	8.56	0.86	1.57	0.43	0.51
K_2O	0.42	0.24	0.92	0.23	0.34	3.78	0.18	1.59	1.12	0.74		1.14	0.83	4.60	1.02	1.11	4.56
P_2O_5	0.02	0.08	0.12	0.02	nf	0.17	nf	0.11	0.14	0.15		0.31	0.04	0.22	0.29	0.01	0.05
H_2O^+	1.24	1.00	2.71	0.48	2.73	4.83	0.28	5.28	1.29	0.64		0.94	0.63	6.08	3.62	1.75	3.36
CO_2	4.92	0.69	1.15	39.8	22.2	1.59	42.6	8.13	2.90	2.02		2.86	0.63	0.14	0.26	0.60	0.18
others	0.26	6.84	7.70	0.06	0.12	0.31	0.09	0.33	0.15	0.14	0.06	0.15	0.25	2.42	8.55	2.77	0.37
O=S	–0.01	–0.54	–0.01	–0.00	–0.01	–0.01	–0.00	–0.05	–0.01	–0.01		0.00	0.00	0.00	–0.00	0.00	0.00
TOTAL	99.2	99.8	100.9	100.9	98.5	100.9	100.3	99.2	100.1	100.4	0.1	99.8	98.7	98.5	98.9	100.7	101.0
Fe_2O_3(T)	1.75	2.31	1.27	1.86	12.2	6.04	0.60	10.7	0.82	0.29		0.64	0.24	0.39	1.41	0.56	0.40
S	300	10800	150	100	300	250	100	1000	150	150		nf	nf	nf	100	nf	nf
Be	1.1	0.9	7.7	0.4	1.0	3.6	0.5	1.5	1.4	1.1			1.2	6.2	8.2	2.6	2.4
Li	22	160	13	nf	3	86	nf	173	23	7		9	nf	56	8	14	15
B	55	38	23200	<25	40	160	<25	50	30	<25	95	55	400	6800	26100	8300	660
Sc	15.3	4.2	30.4	0.9	3.0	20.7	1.0	25.8	16.1	21.0	13.9	12.1	13.6	27.4	29.1	10.0	16.9
V	77	27	233	12	20	188	10	203	164	136		90	129	229	161	111	188
Cr	39	24	176	15	17	125	16	224	115	109	85	65	103	200	4	90	128
Co	1.8	5.0	2.6	3.1	20.3	17.1	0.6	38.0	2.7	1.3	10.0	9.1	1.0	0.6	3.7	1.6	1.1
Ni	36	31	428	nf	46	80	nf	69	87	178		91	55	44	92	32	14
Cu	89	1308	16	7	18	42	5	92	11	9		9	6	9	22	48	19
Zn	702	950	41	16	101	67	16	46	9	6		19	16	23	72	46	19
As	nf	56	nf	4	22	nf	3	30	nf	nf		48	11	7	nf	nf	nf
Rb	30	17	45	10	11	207	nf	86	55	nf		65	40	205	46	52	166
Sr	255	26	73	221	99	70	444	196	210	127		115	126	50	49	26	53
Y	29	4	21	13	38	14	12	17	15	28		26	18	20	22	6	8
Zr	113	17	198	56	51	140	58	103	88	117		99	109	177	206	97	136
Nb	15	3	25	16	10	14	16	4	16	18		11	14	24	17	11	14
Sb	1.9	43.0	2.1	3.0	7.4	2.2	38.0	2.0	2.3	2.2	1.6	4.3	8.1	4.4	2.4	1.5	0.9
Cs	0.9	2.5	2.7	0.7	1.2	15.8	0.4	6.9	3.0	1.5	1.5	6.9	2.6	11.0	2.1	1.9	13.1
Ba	25	17	73	21	49	458	18	70	66	54		100	64	518	126	133	350
La	7.6	4.1	4.0	7.7	27.4	39.7	6.8	8.1	3.8	5.9	21.2	42.1	27.8	7.6	19.0	3.0	4.9
Ce	21.9	9.0	6.3	16.0	47.2	81.4	6.9	19.5	8.3	11.7	56.1	105.0	69.5	17.6	37.0	6.4	11.1
Nd	13.7	3.9	4.8	9.5	26.3	33.6	5.7	11.7	6.6	10.2	31.9	41.5	34.0	11.8	19.3	3.2	5.2
Sm	2.82	0.82	1.34	2.27	8.19	5.25	1.41	2.75	1.98	3.79	9.44	7.70	5.74	3.57	5.06	0.67	1.00
Eu	0.54	0.14	0.37	0.70	3.61	0.88	0.33	0.87	0.29	0.30	0.60	0.80	0.25	0.29	0.38	0.12	0.16
Gd	3.7	0.0	1.8	2.4	8.0	4.4	1.2	nf	2.4	5.7	9.3	9.1	6.2	6.7	7.7	0.0	0.0
Tb	0.60	0.18	0.44	0.35	1.28	0.67	0.22	0.55	0.30	1.18	1.40	1.35	0.80	1.18	0.98	0.12	0.19
Tm	0.47	nf	nf	0.13	0.60	nf	0.07	0.31	nf	0.73	0.56	0.44	0.31	0.64	0.68	0.07	0.21
Yb	3.10	0.42	2.62	0.66	2.45	2.61	0.56	1.85	1.40	4.31	3.42	2.55	2.03	4.31	3.72	0.90	1.58
Lu	0.46	0.05	0.46	0.08	0.35	0.37	0.08	0.25	0.19	0.61	0.54	0.37	0.38	0.59	0.66	0.17	0.23
Hf	2.7	0.5	5.0	0.2	0.2	4.0	0.1	2.0	3.1	3.7	2.4	2.4	3.0	6.1	5.6	2.2	3.8
Ta	0.83	0.17	1.53	0.10	0.10	1.25	nf	0.42	0.97	1.13	0.80	0.76	0.89	1.85	1.92	0.70	1.10
Th	7.10	1.60	15.00	0.60	1.00	13.40	0.40	0.79	9.10	12.90	7.30	8.00	14.00	22.20	19.30	4.20	12.00
U	2.9	0.3	3.2	0.4	1.4	2.7	0.6	0.8	1.8	1.9	1.9	2.2	2.2	3.8	4.3	1.3	1.3
Pb	198	50000	138			15		52	13	10							

Table 4 *contd.*

SAMPLE	SC20B	SC21	47262	47263	47253	DH1	DH4	DH5	DH6	DH7	DH9	DH10	DH11	DHQ3	DHQ5	DHQ6
SiO_2	72.2	62.6	49.6	39.9	56.5	58.6	55.2	49.0	58.8	52.2	64.1	46.7	69.6	70.2	57.3	53.9
TiO_2	0.48	0.65	1.12	1.46	1.05	0.43	0.60	0.74	0.66	0.64	0.74	1.20	0.65	0.61	1.00	0.78
Al_2O_3	12.2	18.5	28.2	32.2	23.6	9.88	15.5	17.6	18.5	12.7	17.8	20.0	17.9	15.8	22.3	19.5
Fe_2O_3	0.20	0.60	0.07	0.20	0.16	0.69	1.00	1.43	0.81	2.45	0.83	1.54	0.49	0.00	0.72	0.35
FeO	0.56	0.17	0.32	0.39	0.13	6.99	3.38	4.29	6.13	6.87	2.09	10.5	0.10	0.26	3.10	2.93
MnO	0.05	0.03	0.02	0.02	0.02	0.09	0.09	0.14	0.05	0.59	0.04	0.04	0.01	0.02	0.05	0.06
MgO	2.70	0.45	5.02	6.43	3.54	3.71	2.13	4.15	2.33	5.07	2.02	5.96	0.07	0.36	2.10	2.94
CaO	1.09	3.24	0.25	0.38	0.42	6.79	4.33	5.21	0.30	5.92	0.19	0.78	0.12	0.72	0.94	3.74
Na_2O	0.61	8.95	1.27	1.64	0.78	0.11	7.35	0.35	5.35	1.96	8.78	3.74	8.91	9.92	5.73	6.77
K_2O	0.58	0.36	2.29	1.63	2.94	1.03	0.60	3.90	1.33	0.95	0.76	1.61	0.37	0.43	2.70	1.52
P_2O_5	0.05	0.11	0.09	0.24	0.16	0.06	0.16	0.13	0.13	0.09	0.13	0.21	0.02	0.09	0.19	0.15
H_2O^+	1.53	0.73	3.27	3.72	4.07	3.51	1.73	4.04	3.49	4.52	1.88	6.14	0.41	0.30	2.63	1.71
CO_2	1.43	3.07	0.87	0.22	nf	7.11	4.62	7.09	0.40	5.07	nf	0.98	0.12	0.86	1.39	5.57
others	3.30	0.26	6.91	9.48	3.83	0.19	0.15	0.44	0.19	0.18	0.17	0.41	0.10	0.08	0.24	0.18
O=S	–0.00	0.00	0.00	0.00	0.00	–0.00	–0.01	–0.10	0.00	0.00	0.00	–0.07	0.00	0.00	0.00	0.00
TOTAL	97.0	99.7	99.3	97.9	97.2	99.2	96.8	98.4	98.4	99.2	99.6	99.7	98.9	99.6	100.4	100.1
Fe_2O_3(T)	0.82	0.79	0.43	0.63	0.30	8.46	4.76	6.20	7.62	10.1	3.15	13.2	0.60	0.28	4.17	3.61
S	100	nf	nf	nf	nf	100	250	2000	nf	nf	<50	1500	nf	nf	nf	nf
Be	2.7	1.5	8.8	10.9	5.6	1.0	1.1	2.8	2.1			3.3			3.2	1.9
Li	13	3	37	41	27	128	73	82	149	143	64	238	4	1	63	42
B	9900	550	20800	28700	11400	50	<25	60	25	30	<25	55	30	<25	70	35
Sc	10.8	15.2	20.3	30.8	25.8	8.4	10.3	17.0	10.0	13.8	15.8	29.7	9.7	10.5	21.0	18.0
V	120	85	202	224	202	91	82	164	173	123	170	234	99	62	201	160
Cr	97	85	133	172	152	70	78	105	100	90	110	338	93	89	139	124
Co	2.7	0.5	0.7	1.1	0.9	22.2	12.6	18.5			35.5	46.5	1.5	4.8	25.2	22.1
Ni	32	14	44	24	45	91	26	133	101	94	81	147	35	32	113	113
Cu	16	11	9	12	8	63	20	33	16	36	6	9	6	3	8	8
Zn	44	41	17	18	16	91	27	74	74	92	18	47	28	1	120	24
As	34	nf	8	12	6	12	11	17	26	47	38		nf	27	29	18
Rb	23	nf	88	75	123	51	23	209	69	41	28	86	nf	13	108	65
Sr	37	166	47	55	40	128	140	95	66	164	111	107	208	129	110	233
Y	9	19	8	11	6	17	16	20	16	21	20	10	7	11	30	17
Zr	71	101	145	200	148	90	92	116	105	93	111	98	109	96	141	116
Nb	10	14	21	28	19	11	12	19	13	15	15	6	13	3	17	14
Sb	2.2	1.1	3.9	3.1	6.4	11.0	4.0	4.6	1.6	4.1	83.0	5.0		3.8	3.2	2.8
Cs	1.0	0.9	3.2	4.0	8.9	2.1	1.7	5.1	3.0	2.8	1.7	9.9		1.8	8.2	3.3
Ba	37	26	598	246	259	77	43	400	99	86	71	150		35	241	112
La	7.6	4.0	52.0	133.0	6.1	42.0	30.4	41.1	46.5	38.8	58.6	9.0		12.4	37.8	28.8
Ce	16.4	12.1	93.6	242.0	9.7	79.3	56.4	74.2	81.0	67.5	100.0	15.7		28.5	102.0	71.0
Nd	7.0	7.9	29.0	85.0	5.2	33.6	24.0	33.9	34.9	30.0	43.4	4.8		14.7	43.3	31.4
Sm	1.43	2.30	2.57	9.60	1.16	5.48	4.18	5.67	5.30	5.34	7.50	2.13		3.03	7.50	5.03
Eu	0.24	0.26	0.23	0.74	0.11	0.94	0.71	1.01	1.03	1.20	0.66	0.50		0.49	1.52	0.86
Gd	0.2	0.0	<2	5.2	<2	4.3	4.9	3.1	nf	nf	6.3	1.1		4.5	6.6	4.2
Tb	0.20	0.57	0.28	0.72	0.15	0.54	0.49	0.51	0.57	0.71	0.96	0.41		0.48	0.90	0.56
Tm	0.12	0.29				0.33	0.21	0.37	0.41	0.37	0.43	0.15		0.26	0.59	0.34
Yb	1.09	1.90	2.72	4.34	1.76	1.55	1.38	2.60	1.64	2.43	2.37	1.35		1.86	3.38	2.57
Lu	0.17	0.30	0.42	0.64	0.29	0.23	0.22	0.38	0.28	0.37	0.33	0.21		0.24	0.48	0.37
Hf	2.2	2.8	4.20	5.70	4.10	1.9	2.6	3.4	3.0	2.9	3.4	2.0	2.7	2.8	4.1	3.4
Ta	0.62	0.88	1.3	1.7	1.2	0.63	0.74	0.80	0.87	0.81	1.04	0.43		0.83	1.30	1.10
Th	9.90	8.40	15.30	22.00	15.40	6.80	8.70	10.50	11.60	8.40	11.30	0.78	8.90	8.40	13.20	10.90
U	1.0	2.0	2.90	3.60	1.30	1.7	1.7	2.4	2.4	1.9	3.3	0.9		1.3	2.8	2.5
Pb	86						19	39	119							

SAMPLE	DHQ7	DHQ8	DHQ9	DHQ10	DHQ11	DHQ12	PC5	PC6	ST1	ST2	ST5	TR1	TR2	TR3	CAT2	CAT3
SiO_2	66.5	67.9	48.8	58.0	87.6	42.9	60.4	41.2	53.2	47.4	62.7	45.3	59.9	57.7	56.6	47.7
TiO_2	0.55	0.63	1.55	0.92	0.49	1.40	0.71	2.76	0.87	1.74	0.79	2.59	0.87	0.81	0.88	2.00
Al_2O_3	16.9	18.6	15.4	20.7	6.32	15.9	14.6	14.2	24.4	17.8	19.6	10.6	23.3	21.8	22.0	16.7
Fe_2O_3	0.00	0.49	1.27	0.55	0.12	0.50	1.42	1.02	2.32	1.29	1.55	1.75	3.36	3.13	1.71	1.79
FeO	0.54	0.16	8.92	3.56	0.68	13.1	5.08	12.0	4.14	7.89	3.45	8.08	0.49	1.77	4.47	11.4
MnO	0.04	0.02	0.17	0.06	0.04	0.20	0.16	0.29	0.05	0.11	0.06	0.13	0.01	0.02	0.06	0.17
MgO	1.14	0.35	4.93	2.74	0.67	9.80	3.49	5.89	2.63	4.34	2.94	9.82	1.30	1.43	2.50	6.13
CaO	2.10	1.09	5.11	0.60	1.11	2.22	1.76	3.87	0.32	6.39	0.19	14.2	0.16	0.90	0.17	9.36
Na_2O	8.74	8.67	3.48	4.28	1.75	0.81	0.51	4.07	0.35	4.83	0.36	2.51	0.41	0.33	3.60	2.84
K_2O	0.40	0.60	1.05	3.50	0.94	1.39	3.30	0.49	6.19	0.44	4.43	0.16	6.24	5.33	3.13	0.15
P_2O_5	0.12	0.26	0.09	0.17	0.11	0.25	0.16	0.65	0.07	0.33	0.07	0.34	0.09	0.08	0.09	0.16
H_2O^+	0.22	0.53	4.31	3.28	1.01	7.21	4.37	4.73	4.95	4.16	4.32	2.45	4.12	4.59	3.99	2.07
CO_2	2.90	1.26	4.06	1.09	0.63	3.19	1.89	3.80	0.29	3.46	0.16	1.84	0.26	1.88	0.15	0.11
others	0.11	0.11	0.51	0.26	0.09	0.42	0.22	0.37	0.19	0.21	0.17	0.23	0.26	0.22	0.19	0.19
O=S	0.00	–0.00	–0.15	0.00	0.00	–0.06	0.00	–0.06	0.00	–0.00	0.00	0.00	0.00	0.00	0.00	0.00
TOTAL	100.3	100.7	99.5	100.2	101.0	99.2	98.0	95.2	99.9	100.4	100.8	100.0	100.8	99.9	99.6	100.8
Fe_2O_3(T)	0.57	0.67	11.2	4.51	0.88	15.1	7.07	14.3	6.92	10.1	5.38	10.7	3.90	5.10	6.68	14.4
S	nf	50	3000	nf	nf	1300	nf	1200	nf	50	nf	nf	nf	nf	nf	nf
Be		1.0	1.5						3.1	1.5	2.9	1.7	3.5	3.4	2.8	0.9
Li	1	5	84	67	14	239	88	181	99	117	102	29	20	40	112	69
B	<25	<25	<25	55	<25	30	75	<25	85	<25	60	<25	200	130	45	<25
Sc	13.0	8.8	31.4	21.8	8.1	29.9	15.7	21.0	19.4	21.8	17.5	67.0	20.6	20.3	22.3	35.4
V	102	86	181	198	82	232	109	204	133	245	119	309	264	182	208	313
Cr	94	118	216	130	97	567	93	102	121	14	104	98	128	130	128	168
Co	2.6	1.3	37.0	28.4	2.6	56.0	22.0	52.0	14.4	25.0	22.6	44.0	32.0	10.4	16.8	43.8
Ni	49	37	25	165	41	175	88	118	40	19	44	84	64	58	69	39
Cu	6	24	44	34	3	51	45	56	10	42	12	108	71	50	17	5
Zn	5	17	55	25	19	94	72	120	59	79	45	61	18	85	53	122
As	35	12	8	47	7	28	11	75	4	5	2	3	63	36	23	4
Rb	13	21	59	147	37	57	135	nf	224	28	193	nf	333	242	153	17
Sr	257	206	537	183	58	54	52	131	24	526	38	468	54	62	45	294
Y	17	27	17	19	6	11	13	30	19	19	11	17	16	13	16	19
Zr	77	108	79	147	78	95	113	225	139	19	133	156	106	112	118	127
Nb	10	11	6	20	9	nf	14	94	16	23	12	27	16	16	16	5
Sb	9.4	4.9	3.4	13.1	3.9	1.3	1.1	2.7	1.5	1.8	1.1	1.0	4.4	2.5	1.8	0.3
Cs	1.1	1.3	9.7	11.2	1.8	3.8	8.4	1.7	9.7	9.4	7.8	0.6	15.3	15.5	9.0	7.4
Ba	44	58	93	325	100	146	434	48								
La	3.8	3.6	6.7	47.2	9.7	6.5	39.4	73.2	50.5	15.1	36.0	24.5	44.1	51.9	47.0	9.6
Ce	15.1	13.1	17.9	94.5	24.7	15.3	84.4	141.0	92.6	31.4	71.5	54.0	89.6	100.0	92.5	20.7
Nd	13.2	10.0	12.4	42.3	14.6	9.4	34.1	55.4	35.4	16.1	31.7	31.8	41.0	38.3	38.5	16.4
Sm	3.24	2.88	3.21	7.77	2.48	2.70	6.20	9.70	5.74	3.82	5.19	7.49	6.79	5.37	5.85	4.00
Eu	0.42	0.52	1.17	1.38	0.28	0.60	1.32	2.63	1.15	1.54	1.04	2.47	1.12	0.84	1.24	1.70
Gd	0.0	5.3	0.0	7.0	nf	nf	5.6	7.7	6.9	2.2	5.1	5.1	4.7	5.0	6.1	3.7
Tb	0.48	0.80	0.64	1.01	0.24	0.58	0.74	1.08	0.79	0.63	0.67	1.03	0.78	0.55	0.62	0.71
Tm	0.25	0.44	0.33	0.62	0.16	0.27	0.35	0.61	0.39	0.16	0.35	0.27	0.35	0.39	0.39	0.35
Yb	1.69	2.72	1.90	3.46	0.88	1.78	2.54	2.45	2.92	1.56	2.49	1.42	3.02	2.42	2.65	1.82
Lu	0.21	0.38	0.27	0.49	0.11	0.22	0.33	0.31	0.40	0.22	0.36	0.16	0.45	0.35	0.36	0.27
Hf	2.5	2.7	2.2	4.1	2.2	2.0	3.7	6.5	3.5	2.8	3.8	5.4	3.7	3.8	3.9	3.1
Ta	0.64	0.90	0.41	1.07	0.64	0.37	1.00	5.80	1.10	1.20	1.00	2.00	1.20	1.00	1.00	0.50
Th	6.90	7.20	0.67	12.40	6.80	0.48	10.00	9.00	13.70	1.70	11.70	2.50	14.00	13.60	14.10	0.60
U	2.3	1.9	0.2	2.8	1.2	0.2	1.7	2.6	2.1	0.5	3.4	0.7	2.8	2.7	2.4	0.3
Pb									19	64	39	22	19	40		

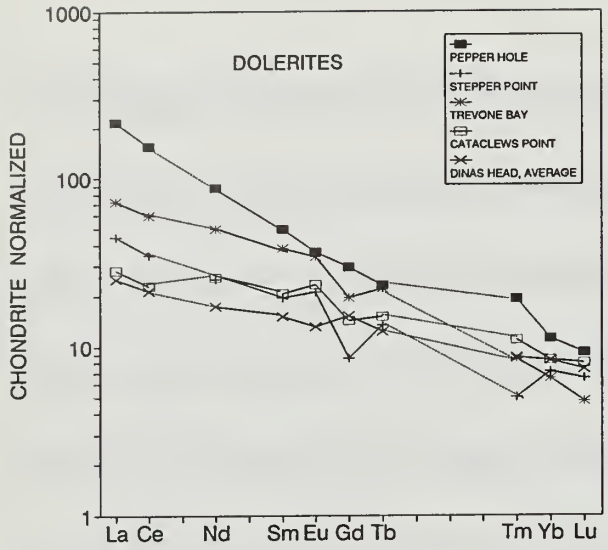

Fig. 4 Chondrite normalised REE plots for the dolerites. The Dinas Head plot is the average of six samples.

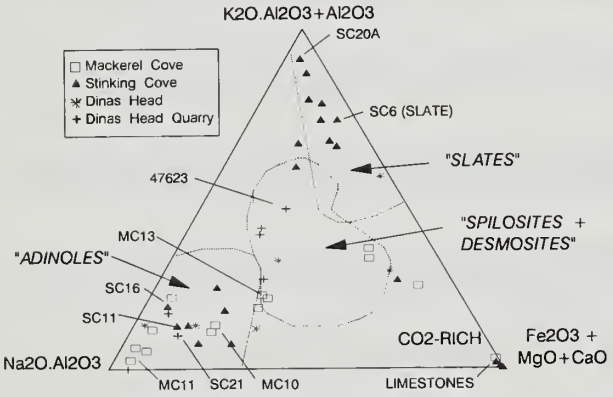

Fig. 5 Ternary diagram (modified after Agrell, 1939) delineating fields for 'adinole', 'spilosites + desmosites' and 'slate'. Samples plotted are all the Dinas Head sediments, and those labelled are referred to in the text.

field, albite is a major mineral phase, whereas mica and chlorite are predominant in sediments from the 'slate' field. It is also noteworthy that true 'adinoles' occur in all 4 sections sampled, illustrating the extensive distribution of adinoles at Dinas Head. Samples rich in CO_2 plot towards the (Fe_2O_3+FeO+MgO+MnO+CaO) apex of the ternary diagram.

Sediments from the Stinking Cove section appear to differ from those of the other sections in that they plot either as true adinoles (e.g. SC11 and SC16), or in the 'slate' field of the ternary diagram (e.g. SC20A, Fig. 5). All of the samples in the 'slate' field are boron-rich, although some adinoles at Stinking Cove are also boron-rich (e.g. SC21, NA_2O = 8.95%, B = 550 ppm), but with lower boron concentration levels. It appears likely that the introduction of boron was concomitant with removal of sodium.

The sample of unaltered fissile slate collected from the Stinking Cove section (SC6) plots well within the 'slate' field. Slate samples collected well away from the intrusive dolerites at Stepper Point (ST5) and Trevone Bay (TR3), also plot very close to the Dinas Head slate sample on all the geochemical diagrams presented (e.g. Figs 6, 10 and 11).

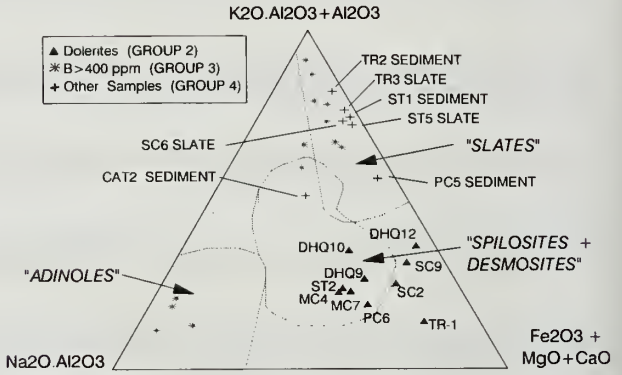

Fig. 6 Apices as for Fig. 5. Samples plotted are: dolerites — GROUP 2 (filled triangles); sediments with B>400 ppm — GROUP 3 (stars); sediments associated with dolerites from other N Cornwall localities (crosses).

Sediments associated with dolerites from Stepper Point, Pepper Hole and Trevone Bay do not show any chemical indications of adinolisation, and plot in the 'slate' field (Fig. 6). However, the sediment associated with the dolerite from Cataclews Point plots in the 'spilosite + desmosite' field, and may well indicate that some degree of sodium mobility had occurred.

Sediments with Na_2O >4%, i.e. those which plot in the 'adinole' or 'spilosite + desmosite' fields, were classified as GROUP 1 sediments in all following diagrams. The REE contents vary for this group, and are plotted as chondrite-normalised values in Fig. 7 in the field delineated by ±1 standard deviation of the mean of these values. In general, the GROUP 1 sediments are light-REE enriched with a prominent negative Eu anomaly. The unaltered slate (SC6) is shown for comparison in Fig. 7, and has a similar pattern to that of the GROUP 1 sediments, although REE concentrations are slightly higher than the GROUP 1 mean. GROUP 3 sediments, i.e. those with boron greater than 400 ppm, are similarly light-REE enriched, but generally with a larger negative Eu anomaly (Fig. 8). Sediments rich in CO_2 generally have flatter chondrite-normalised patterns, with positive, or less negative, Eu anomalies (Fig. 9).

All analytical data, including the dolerites, are plotted on Taylor and McLennan's (1985) ternary diagrams Hf-Th-Co (Fig. 10), and Th-La-Sc (Fig. 11), which are used to discriminate post-Archean sediments. The unaltered slates, together with those sediments in close proximity to dolerites *other than* the Dinas Head intrusion, plot within the post-Archean sedimentary fields on both ternary diagrams. These samples, together with the CO_2-rich sediments and the quartz-granite veins (SC2 and DHQ11), are classified as GROUP 4 samples. Many of the Dinas Head sediments however, plot outside the post-Archean sedimentary fields on both diagrams. In the Hf-Th-Co diagram, Fig. 10, the variation is greatest, as both GROUP 1 and GROUP 3 sediments plot on either side of this field. In the Th-La-Sc diagram, Fig. 11, the sediments are better delineated, with the majority of sediments in GROUPs 1 and 3 plotting within the post-Archean sedimentary field.

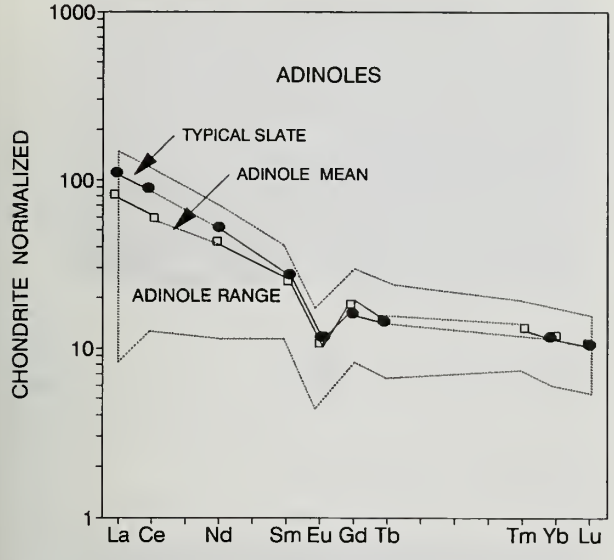

Fig. 7 Chondrite normalised REE plots for the range of adinoles from Dinas Head.

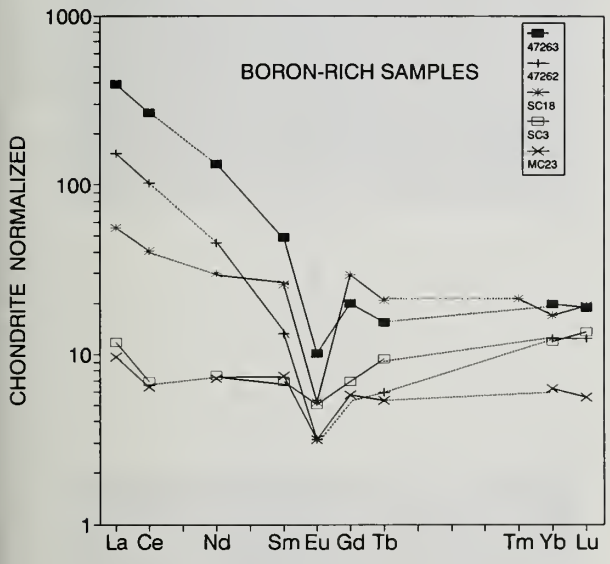

Fig. 8 Chondrite normalised REE plots for selected boron-rich sediments.

Samples plotting outside this field are predominantly boron-rich, and are relatively depleted in La.

The CO_2-rich samples at Stinking Cove (SC4, SC5 and SC7) plot together but separate from the other samples in the Th-La-Sc diagram (Fig. 11), and are distinct from the CO_2-rich samples at Mackerel Cove (MC5, MC6, MC8 and MC9). This difference is due to an enrichment of Sc (relative to La) which correlates with an observed greater abundance of Fe-carbonate (siderite) at Mackerel Cove.

In both ternary diagrams (Figs 10 and 11), the dolerites form a group which generally is distinct from the sediments.

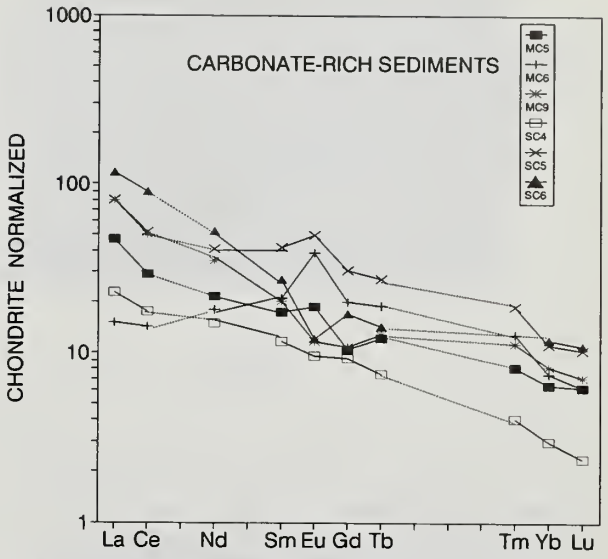

Fig. 9 Chondrite normalised REE plots for carbonate-rich rocks.

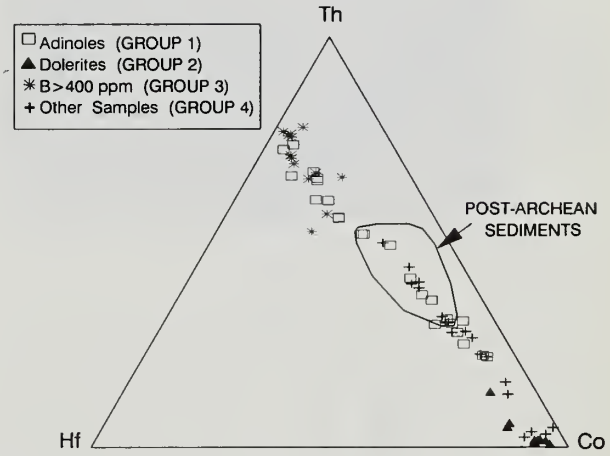

Fig. 10 Ternary diagram, after Taylor and McLennon (1985). Samples plotted are: adinoles — GROUP 1 (open squares); dolerites — GROUP 2 (filled triangles); sediments with B>400 ppm — GROUP 3 (stars); other samples — GROUP 4 (crosses).

Boron-rich samples

Agrell (1939, 1941) provides an excellent comprehensive textural and mineralogical description of the boron-rich samples from Dinas Head, where he identified dravite to be the sole boron-bearing mineral. Here, we analysed several samples using x-ray diffractometry and can confirm that dravite is the tourmaline mineral present. Our mapping of the sediments indicates that the boron mineralisation has a very localised areal distribution, as reported by Agrell (1939), and is confined to the top of the Mackerel Cove and Stinking Cove sedimentary sequences (Fig. 1). In thin section it was not possible to identify the tourmaline because of the small grain size of the minerals present; scanning electron microscopy showed the grain sizes to be typically less than 1 μm, Figs 3(c),(d).

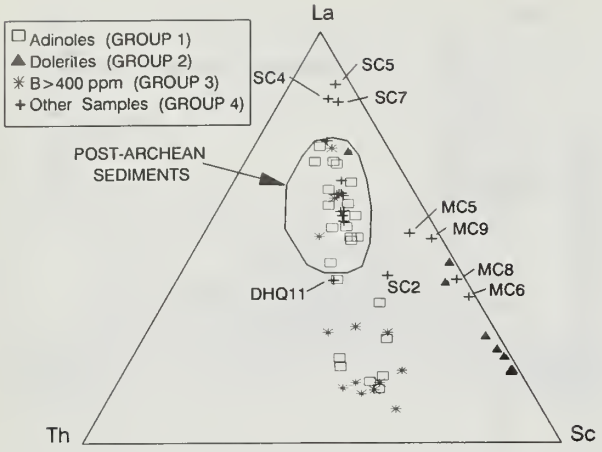

Fig. 11 Ternary diagram, after Taylor and McLennon (1985). Samples plotted are: adinoles — GROUP 1 (open squares); dolerites — GROUP 2 (filled triangles); sediments with B>400 ppm — GROUP 3 (stars); other samples — GROUP 4 (crosses).

In the ternary diagrams, Figs 6, 10 and 11, samples with boron concentration greater than 400 ppm are classified as boron-rich (GROUP 3). From the ternary diagram $(Na_2O.Al_2O_3) - (K_2O.Al_2O_3) - (Fe_2O_3 + FeO + MgO + MnO + CaO)$, Fig. 6, originally used in Agrell's (1939) classification of adinoles, it can be seen that the boron-rich samples are not confined to any specific rock type, suggesting that the boron mineralisation post-dates the adinolisation metasomatic event. From the Th-La-Sc and Hf-Th-Co ternary diagrams, Figs 10 and 11, the boron-rich samples generally are depleted in Co, and to a lesser extent La, and a crude inverse correlation exists between these two elements and boron (Fig. 12). Chondrite normalised REE plots show a wide range for the light-REE, but are not significantly different from the boron-poor sediments, except generally to have larger negative Eu anomalies (Fig. 8). No significant correlations were observed for the other elements studied. Neither the dolerite nor the unaltered slate are enriched in boron and are unlikely to be the source for the mineralisation, and no boron-rich samples occurred with sediments associated with dolerites from the other areas in this study.

Boron Isotopes

The boron isotope signatures of an adinole sample from Stinking Cove (SC18), a tourmaline from Luxulyan, Cornwall (BM68598) and a colemanite (non-marine evaporite) from San Bernadino County, California (BM69058) were measured in an attempt to identify a source from which the boron may have been introduced.

The $\delta^{11}B$ value determined for adinole specimen SC18, referred to National Bureau of Standards boric acid SRM951 ($^{11}B/^{10}B$ ratio 4.04362, Catanzaro *et al.* (1970)) is 5.26‰. This value falls within the field of non-marine evaporites and at the low end of the ranges quoted for sediments and crustal rocks, as summarised by Palmer and Slack (1989). The $\delta^{11}B$ value of pegmatitic tourmaline from Luxulyan, Cornwall, was found to be 12.61‰ and that of the colemanite was found to be 5.13‰. Both lie broadly within the respective ranges for pegmatites and marine evaporites suggested by Swihart and Moore (1989) and Palmer and Slack (1989). According to the latter, seawater and marine evaporites are characterised by $\delta^{11}B$ of +20 to +40‰ whilst Swihart and Moore (1989) reported that pegmatitic tourmalines are depleted in the heavier isotope such that $\delta^{11}B$ is between 5 and 12‰.

Our limited data indicate that neither seawater nor marine

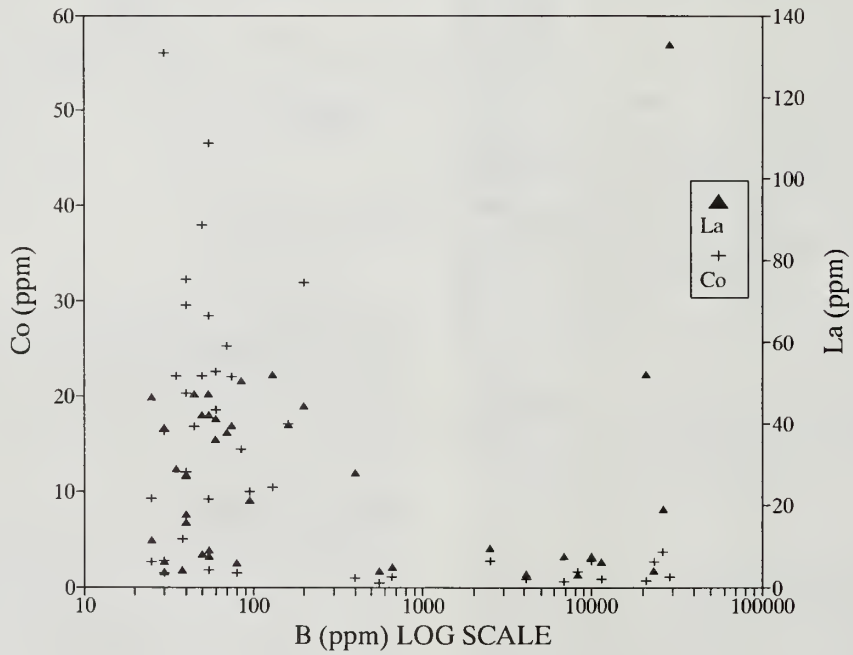

Fig. 12 B against La (filled triangles), and B against Co (crosses).

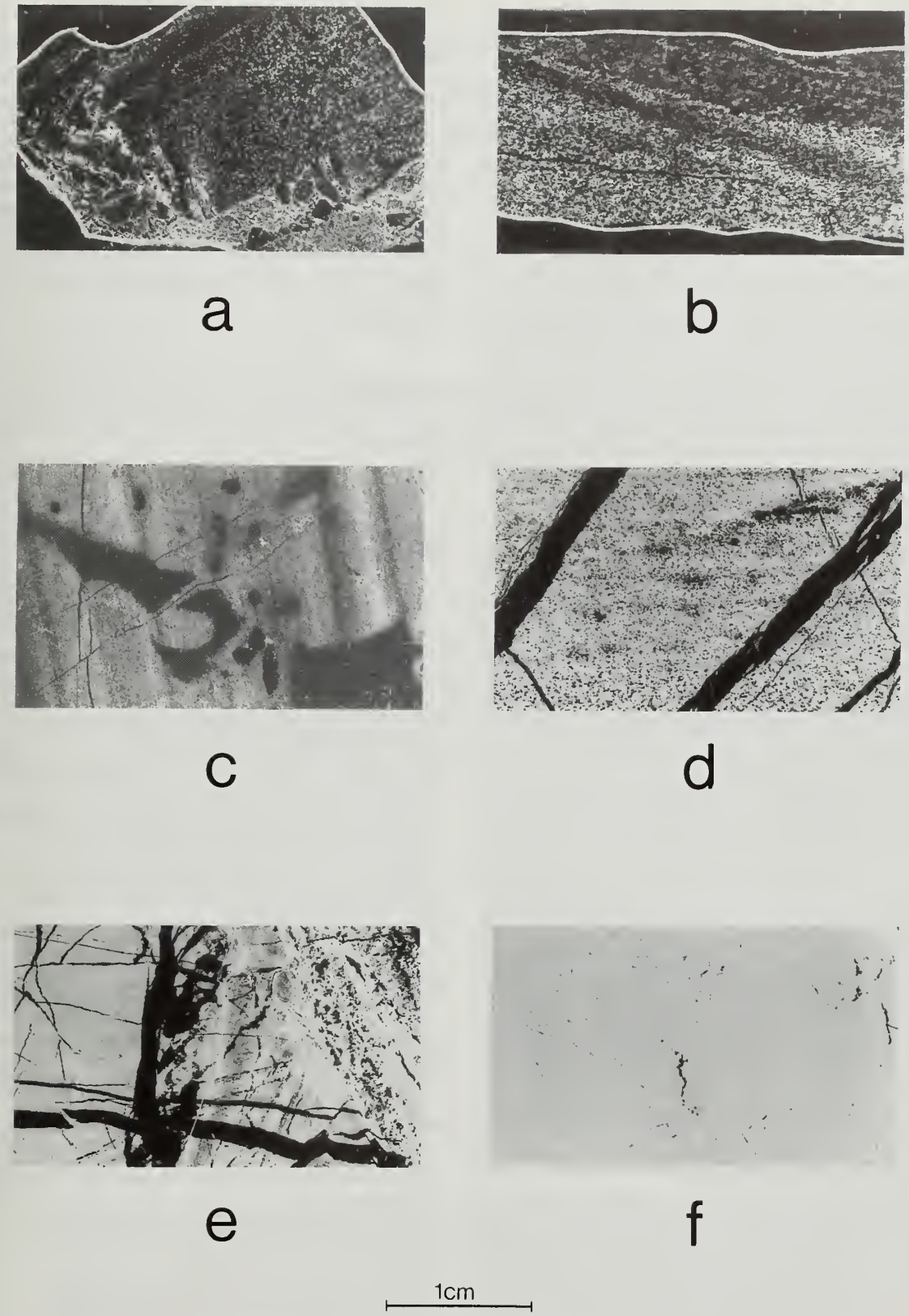

Fig. 13 Boron distribution maps of samples from Stinking Cove. (a) Sample number SC20A (660 ppm B); (b) SC17 (6800 ppm): (c) SC21 (550 ppm); (d) SC20B (9900 ppm); (e) SC19 (5300 ppm); (f) SC18 (25200 ppm).

evaporites could have been the source of the boron introduced during tourmalinisation of the rocks at Stinking Cove. Pneumatolytic fluids may have been involved but the measured ^{11}B depletion of the Cornish pegmatitic tourmaline is sufficiently greater than that of the adinole to indicate that this was not the case. None of the sediments that we examined from the area was found to contain boron at a concentration high enough to suggest that it may have been the source of the element.

Boron Mapping

Boron maps of six adinole samples are illustrated in Fig. 13. Usually, the boron, irrespective of its concentration, is homogeneously distributed throughout the bulk of the specimens, except where zones of post-tourmalinisation mineralisation occur. There is no evidence (such as boron-rich veins) to indicate the mechanics or pathways of boron ingress. Since the boron content of local unaltered slates is unexceptional (about 160 ppm, Shaw and Bugry, 1966) these rocks are unlikely to have been the source of the boron required for the tourmalinisation.

CONCLUSION

This study confirms Agrell's (1939) observations regarding the extensive areal distribution of adinoles at Dinas Head, north Cornwall. Albite-rich adinoles and spilosites extend from the most westerly point at Dinas Head through to the quarry section approximately 500 m east. The majority of samples studied in the Stinking Cove section showed, in addition to the Na-enrichment of normal adinoles, a significant degree of K-enrichment with mica and/or sericite being abundant. It is likely that a hitherto unrecognised phase of K-metasomatism had occurred together with the Na-metasomatism characteristic of adinole formation.

It was not possible to identify all the other elements affected by the adinolisation process because of the probable heterogeneous nature of the original sediments, and thereby lack of a control 'sample'. However, use of Taylor and McClennan (1985) discriminant diagrams for the elements Hf, Th, Co, La and Sc, and chondrite-normalised plots for the REE, indicate that La (and other light REE) were removed, and Th introduced during adinole formation.

It was not possible also to affirm or refute, from the geochemical and petrological data, the generally accepted view that the dolerite was the source of the Na (and/or K) in the formation of the adinoles. The chemical composition of the dolerite at Dinas Head is not significantly different from that of other dolerites in the area where adinoles were *not* observed at the dolerite/sediment contacts. However, the plagioclase present in the Dinas Head dolerite proved to be near end-member albite, some of which appeared to be primary in origin, and may well therefore have been associated with the adinolisation process.

Boron-rich samples, with boron in excess of 2%, were observed locally at Dinas Head, being restricted to the upper regions of the Stinking Cove section, and to the top of the Mackerel Cove section, close to a major fault zone cutting the northern part of the sequence. Dravite was identified as the sole boron mineral. The source of the boron was not identified, but it was unlikely to have been either the dolerites or the unaltered shales. Boron isotope data were inconclusive, indicating neither sea-water nor marine evaporites as the source of the boron. The isotopic ratio of a tourmaline from a Cornish pegmatite was also significantly different from that of the boron-rich sediment at Dinas Head.

The data presented here, and conclusions reached, are not in disagreement with Agrell's (1939) original hypothesis regarding formation of the adinoles at Dinas Head by metasomatic fluids emanating from the dolerite. We were not able however, to confirm this hypothesis. In addition, our observations are consistent with Agrell's (1941) hypothesis of tourmaline formation as a separate event, later than the adinolisation process. Thus while we were not able to ascertain conclusively the precise mechanisms of Na, K and B metasomatism at Dinas Head, this study provides a useful database against which studies of rocks of a similar nature can be compared.

ACKNOWLEDGEMENTS. We are very grateful to Dr. R.C. Scrivener (British Geological Survey, Exeter) and Dr. A.M. Clark (The Natural History Museum, London) for comments on an earlier manuscript.

REFERENCES

Agrell, S.O. 1939. The adinoles of Dinas Head, Cornwall. *Mineralogical Magazine*. **23:** 305–337.

—— 1941. Dravite-bearing rocks from Dinas Head, Cornwall. *Mineralogical Magazine*. **26:** 81–93.

Catanzaro, E.J., Champion, C.E., Garner, E.L., Marinenko, G., Sappanfield, K.N. & Shields, W.R. 1970. *Boric Acid; Isotopic and Assay Standard Reference Materials*. United States National Bureau of Standards Special Publication 260–17, 70pp.

Dewey, H. 1915. On spilosites and adinoles from north Cornwall. *Transactions of the Royal Geological Society of Cornwall*. **15:** 71–84.

Din, V.K. & Jones, G.C. 1978. The determination of total carbon and combined water in silicates, using a C,H,N elemental analyser. *Chemical Geology* **23:** 347–352.

—— **and Henderson, P.** 1982. Application of CR-39 to the mapping of B in minerals and rocks. *In* Fowler, P.H. & Clapham, V.M. (eds). *Solid State Nuclear Track Detectors*. Oxford (Pergamon Press): 958pp.

Floyd, P.A. 1982. Chemical variation in Hercynian basalts relative to plate tectonics. *Journal of the Geological Society, London*. **139:** 505–520.

Fox, H. 1895. On a soda feldspar rock at Dinas Head, North coast of Cornwall. *Geological Magazine*. **II:** 13–20.

French, W.J. & Adams, S.J. 1972. A rapid method for the extraction and determination of iron(II) in silicate rocks and minerals. *Analyst (London)* **97:** 828–831.

Kayser, E. 1870. Ueber die Contactmetamorphose der körnigen Diabase im Harz. *Zeitschrift der Deutschen Geologischen Gesellschaft. Berlin*. **22:** 103–172. [In German].

McMahon, C.A. & Hutchings, W.M. 1895. Note on pseudo-spherulites. *Geological Magazine*. **II:** 257–259.

Palmer, M.R. & Slack, J.F. 1989. Boron isotopic composition of tourmaline from massive sulfide deposits and tourmalinites. *Contributions to Mineralogy and Petrology*. **103:** 434–451.

Swihart, G.H. & Moore, P.B. 1989. A reconnaissance of the boron isotopic composition of tourmaline. *Geochimica et Cosmochimica Acta*. **53**: 911–916.

Shaw, D.M. & Bugry, R. 1966. A review of boron sedimentary geochemistry in relation to new analyses of some North American shales. *Candian Journal of Earth Sciences*. **3**: 49–63.

Taylor, S.R. & McLennon, S.M. 1985. *The Continental Crust: Its Composition and Evolution*. Blackwell Scientific Publications, Oxford, 312pp.

Teall, J.J.H. 1888. *British Petrography: with Special Reference to the Igneous Rocks*. Dulan & Co., London, 469pp.

Williams, C.T. & Wall, F. 1991. An INAA scheme for the routine determination of 27 elements in geological and archaeological samples. *In* Hughes, M.J., Cowell, M.R. & Hook, D.R. (eds). *Neutron Activation and Plasma Emission Spectrometric Analysis in Archaeology: Techniques and Applications*. British Museum Press, London. British Museum Occasional Paper 82, 106–119.